ABSTRACT

Title of Thesis: COMPARISON OF NEUTRON NON DESTRUCTIVE METHOD AND CONVENTIONAL CHEMICAL METHOD FOR CHLORIDE MEASUREMENT IN CONCRETE

Preethi Sridhar, Master of Science, 2019

Thesis Directed By: Professor, Amde M Amde, Civil and Environmental Engineering

The presence of chloride in concrete is a critical issue raising concerns in the construction industry as they promote corrosion of the steel reinforcements, drastically reducing the strength of the structure. The aim of this study is to compare the performance of a neutron-based nondestructive testing method, Prompt Gamma Activation Analysis (PGAA) against the destructive wet chemistry method ASTM C-1152 currently used to determine the chloride concentration in concrete. Two modes of PGAA operation were tested. One was to use PGAA with a slit collimator to measure the chlorides at 2 mm thick cross-section in intact samples. The other was a direct comparison with C-1152 to analyze powdered concrete samples. Concrete was prepared in four batches, in which three batches had added chloride -at nominally 0.2%, 0.1%, 0.01% by weight of cement and the fourth (control) batch has zero added. The PGAA analysis was done at the Cold Neutron PGAA station at NIST and the C1152 testing was done at the National Ready

Mixed Concrete Association (NRMCA) laboratory. The intact samples were scanned at three different vertical positions.

The PGAA method is capable of detecting Cl at levels corresponding to the corrosion threshold of 0.1-0.2% Cl by weight of cement. The minimum detectable limit for PGAA is below 0.02% Cl by weight of cement and approaches the Cl background contributed by the raw materials, in this case, the cement. The PGAA- measured chlorides concentrations showed excellent linearity after correction for the chloride content in the concrete raw materials, mainly the cement. For the powdered samples, the C1152 and PGAA results were in very good agreement. However, the PGAA data showed much less scatter with an uncertainty as low as 0.3%. The findings of this study indicate that PGAA is a feasible replacement for the C1152 method and since it can be done on intact specimens, it avoids the time-consuming steps of crushing, sieving and nitric acid extraction and can be more cost-effective.

COMPARISON OF NEUTRON NON DESTRUCTIVE METHOD AND CONVENTIONAL CHEMICAL METHOD FOR CHLORIDE MEASUREMENT IN CONCRETE

by

Preethi Sridhar

Thesis submitted to the Faculty of the Graduate School of the
University of Maryland, College Park, in partial fulfillment
of the requirements for the degree of
Master of Science
2019

Advisory Committee:
Professor Amde M Amde, Chair
Professor Mohamad Al-Sheikhly
Professor M Sherif Aggour

Preface

This master thesis is submitted to University of Maryland (UMD), College Park, as a partial fulfillment of the requirements for the degree of Master of Science (MS).

One half of the work has been carried out at the National Ready Mix Concrete Association (NRMCA) in College Park, MD. This work included the preparation of test samples and the analysis of C1152.

The other half of the project was done at the NIST Center for Neutron Research, part of the National Institute of Standards and Technology, Gaithersburg, MD. This included the neutron beam analysis on the specimens and the raw materials.

This project was done under the supervision of Professor Amde M Amde and Professor Richard A Livingston (UMD), Stuart Sherman (NRMCA) and Heather Chen-Mayer (NCNR-NIST).

The project started in August 2018 and completed for submission in May 2019.

Dedication

To my parents, family and partner

For teaching me to believe in myself, my dreams and in God and for the constant moral and emotional support. Thank you for not giving up on me ever.

Acknowledgements

I would first like to thank my thesis advisor Professor **Amde M Amde** of the Civil and Environmental Engineering Department at University of Maryland. I am grateful for his immense interest in my thesis, his valuable advice during topic discussion, for finding time in his busy schedule, for being a constant source of motivation and for introducing me to Prof. Richard Livingston. I am highly indebted to Prof. Amde as this paper would have been impossible without him.

I am grateful to my guide Adjunct Professor **Richard A Livingston** of the Materials Science and Engineering Department at University of Maryland, for his expertise, understanding and vision. I am indebted to him for helping me shape up the project, providing me with relevant materials that I possibly could not have discovered on my own and for his kind words and suggestions. He allowed this paper to be my own work, but steered me in the right direction when required.

I am also thankful to Professor **Sherif M Aggour** of the Civil and Environmental Engineering Department and Professor **Mohamad Al-Sheikhly** of the Material Sciences and Engineering Department at University of Maryland for consenting to be in the committee and for allocating their time.

Special Mention:

I would like to thank **Stuart Sherman**, **RJ Hong** and **Danny Dickerson** from NRMCA. It was great to have the opportunity to work part of my research in your facilities.

I would also like to thank **Heather Chen-Mayer** and **Rick L Paul** from NIST. It was a lifetime opportunity to work with the neutron beam and this project wouldn't have been possible without your constant assistance and valuable inputs.

I am also grateful to my friends who have made this difficult journey an incredible, enriching and fun experience.

Table of Contents

List of Tables

List of Figures

List of Equations

List of Abbreviations

AASHTO	American Association of States Highway and Transportation Officials
ASCE	American Society of Civil Engineers
ASTM	American Society of Testing and Materials
BGO	Bismuth Germanium Oxide
CA	Coarse Aggregate
CDF	Capillary suction of De-icing solution and Freeze thaw
DC	Direct Current
FA	Fine Aggregate
NDT	Non Destructive Testing
NGD	Neutron Guide
NIST	National Institute of Standards and Technology
NRMCA	National Ready Mix Concrete Association
NT	Nord Test
PGAA	Prompt Gamma Activation Analysis
PGNA	Prompt Gamma Neutron Activation
PSI	Pound per Square Inch
RC	Reinforced Concrete
RCPT	Rapid Chloride Permeability Test
RH	Relative Humidity
RMT	Rapid Chloride Migration Test
SRM	Standard Reference Materials
VT	Vertical beam Tube

List of Chemical Abbreviations

Cl^-	Chloride ion
$CaCl_2$	Calcium Chloride
$Ca(HCOO)_2$	Calcium Formate
$Ca(NO_3)_2$	Calcium Nitrate
$Ca(OH)_2$	Calcium Hydroxide
CH	Methylidyne / Carbyne
C_3S	Tricalcium Silicate
C-S-H	Cesium Hydride
Ca_3SiO_5	Calcium Silicate
$Fe(OH)_2$	Ferrous Hydroxide
$Fe(OH)_3$	Ferric Hydroxide
$FeCl_2$	Ferrous Chloride
HCl	Hydrochloric Acid
NaCl	Sodium Chloride
NaOH	Sodium Hydroxide
$NaNO_3$	Sodium Nitrate
AgCl	Silver Chloride
AgOH	Silver Hydroxide
Ag_2O	Silver Oxide
SiO2	Silicon dioxide
$CaCO_3$	Calcium Carbonate

CHAPTER 1: INTRODUCTION

1.1 Objective

The aim of this study is to compare performance of a neutron-based nondestructive testing method, Prompt Gamma Activation Analysis (PGAA) against the destructive wet chemistry method ASTM C-1152 currently used to determine the chloride concentration in concrete. Concrete samples will be prepared to be analyzed in both methods and results will be compared to verify that the non destructive method will be feasible.

1.2 Background

The discovery of concrete was considered revolutionary as it could harden quickly into a rigid mass and unlike the stone or brick, has comparatively less thrust and strain. Concrete is a composite material comprising of coarse and fine aggregates bonded together with cement paste and hardens over time. Concrete can vary based on the binders, aggregates and the requirement. The raw materials used in concrete determine the strength, durability, density and resistance to external factors of the structure. Concrete provides excellent fire resistance and longer service life compared to other materials and gains strength over time.

Cement is generally used as a binder, which, when mixed with aggregates and water, chemically reacts to form slurry that is durable and easily moldable. Aggregates refer to coarse gravel or crushed rocks and sand. Mostly, additives like chemical admixtures, superplasticizers and accelerators are added to the mixture to improve the

physical properties. From the last century, concrete is braced with reinforcing materials to provide tensile strength.

1.3 Hydration of Concrete

Curing is important for the development of strength and durability of concrete. It is done over extended periods of time at a depth and on the surface of the concrete at controlled moisture and temperature. During curing, the process of combining cement with water to form a cement paste occurs and is known as hydration. This is one of the important steps in concrete formation as this paste is responsible to bind the aggregate together, fill voids and make it flow more freely. It involves a series of reactions taking place simultaneously:

$$C_3S + H \rightarrow C\text{-}S\text{-}H + CH$$

$$Ca_3SiO_5 + H_2O \rightarrow (CaO)\cdot(SiO_2)\cdot(H_2O)(gel) + Ca(OH)_2$$

$$2Ca_3SiO_5 + 7H_2O \rightarrow 3(CaO)\cdot2(SiO_2)\cdot4(H_2O)(gel) + 3Ca(OH)_2$$

Equation 1: Hydration of Concrete

The first three days are very critical in the hydration process as it determines the strength of the mix. The mix attains over 90% of its strength during this period and makes it more resistant to damage. The concrete should be kept damp during the curing process to attain increased strength. Minimizing stress prior to curing minimizes cracking. When properly cured, concrete will retain moisture for prolonged hydration. This results in strength development, freeze-thaw resistance, resistance to scaling, volume stability, and abrasion resistance.

1.4 Electrochemical Process

When concrete is exposed to periodic wetting and drying, there will be difference in the regular environment inside the concrete. This leads to differential electrochemical potential along the steel in concrete, where an electrochemical cell is set up connected by the electrolyte in the form of the pore water in the hardened cement paste. The positively charged ferrous ions at the anode pass into electrolyte solution while the negatively charged free electrons pass through the steel into the cathode. They combine with water and oxygen to form hydroxyl ions. The hydroxyl ions travel through the electrolyte and combine with the ferrous ions to form ferric hydroxide, which oxidizes to rust. The reactions involved are as follows:

At Anode:

$$Fe \longrightarrow Fe^{2+} + 2e^{-}$$

$$Fe^{2+} + 2OH^{--} \longrightarrow Fe(OH)_2$$

$$4Fe(OH)_2 + O_2 + 2H_2O \longrightarrow 4Fe(OH)_3$$

Equation 2: Electrochemical Reaction at Anode

At Cathode:

$$O_2 + 2H_2O + 4e^{--} \longrightarrow 4OH^{-}$$

$$Fe^{2+} + 2Cl^{--} \longrightarrow FeCl_2$$

$$FeCl_2 + H_2O \longrightarrow Fe(OH)_2 + 2HCl$$

Equation 3: Electrochemical Reaction at Cathode

Oxygen and water are essential for the process to continue and hence the possibility of corrosion in dry concrete is really low. If the concrete is fully immersed in water or if the relative humidity in concrete is less than 60%, then there would be no

corrosion. For corrosion to be present, the protective layer on the steel must be penetrated. Corrosion results in the increase of corrosion causing agents, decreasing the cross section of steel. This leads to cracking, spalling or delamination of concrete and the load bearing capacity of the concrete.

1.5 Transportation of Chloride Ions

Chloride ions penetrate concrete through diffusion, hydrostatic pressure or capillary absorption. Diffusion refers to the movement of chloride ions under a concentration gradient and this is the most common method of penetration. This occurs when concrete has a constant flowing liquid phase and chloride ion concentration gradient. In rare cases, there would be an applied hydraulic head on one face of the concrete, which would allow chloride to permeate into the concrete. Penetration can also occur by absorption due to cyclic wetting and drying of the concrete surface. Water will be drawn into the porous concrete structure though capillary suction when it encounters a dry surface. This method is possible only if the concrete is of extremely poor quality or if the rebar is shallow.

1.6 Chloride Threshold Limit

The chloride limit allowed in reinforced concrete is one of the important factors to be considered when studying the chloride penetration. The critical chloride content is defined as the total chloride content relative to the weight of the cement. ACI 318 Building code specifies the values to be met for mix proportions considering chloride inclusion. Figure 1 show the chloride threshold values as specified by ACI.

Type	Exposure	Chloride Ion Content in Concrete, % by weight of cement	
		Reinforced Concrete	Prestressed Concrete
Water Soluble	Concrete Dry or Protected from Moisture	1	0.06
	Concrete exposed to moisture but not to external sources of chlorides	0.3	0.06
	Concrete exposed to moisture and an external source of chlorides	0.15	0.06
Acid Soluble	ASTM C 1152	0.1	0.08

Figure 1: Chloride Threshold Limit

This research also takes into consideration the critical chloride limits mentioned in various studies across the world. The paper 'Critical Chloride Content in Reinforced Concrete — A Review' (2009) by Ueli Angst, Bernhard Elsener, Claus K. Larsen and Øystein Vennesland summarizes the findings of all the research available on the threshold limit of chloride under both outdoor and laboratory conditions where steel is embedded in cement. The authors have also summarized the critical limits of total and free chlorides or Cl^-/OH^- ratios as available in various publications. Figure 2 summarizes the chloride threshold values discussed by in different authors.

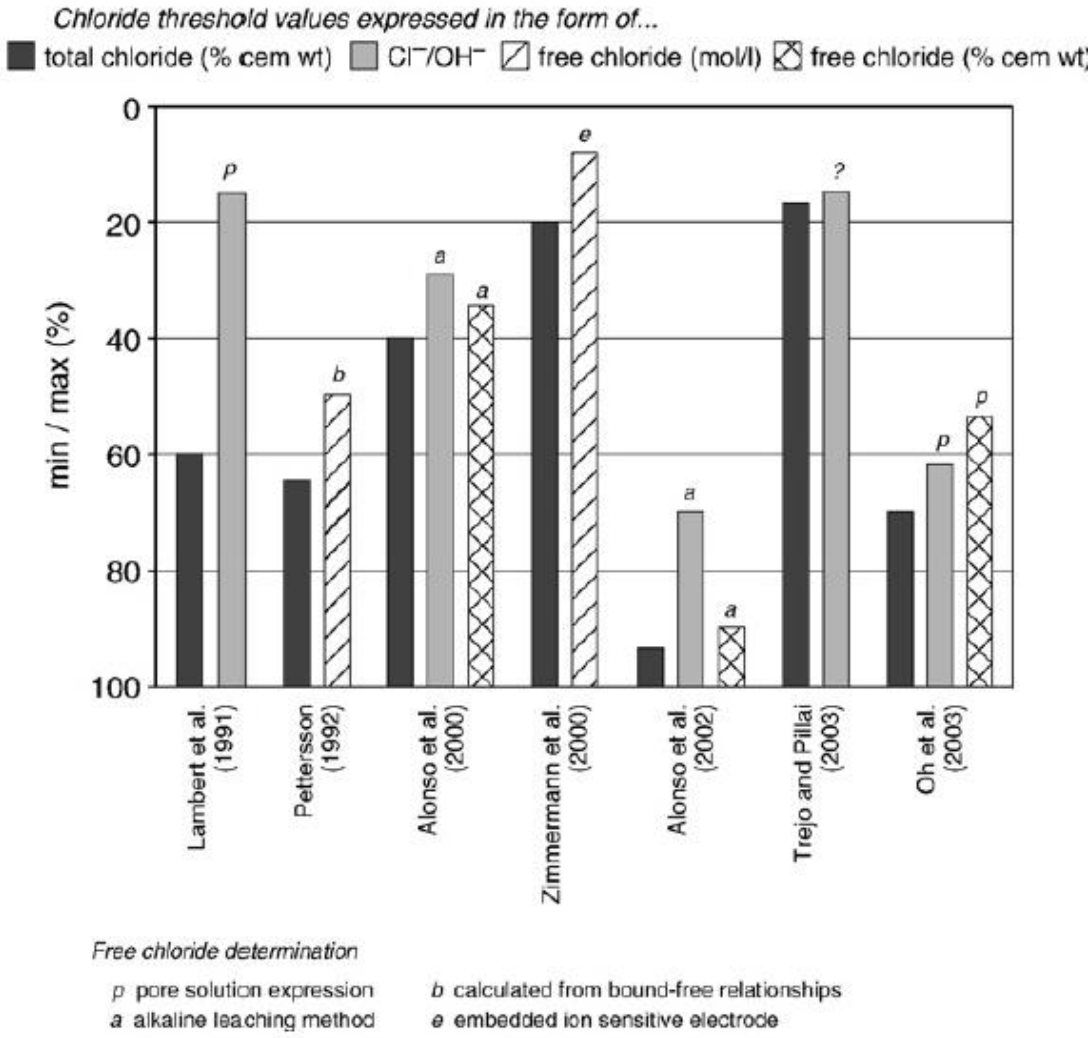

Figure 2: Summarized Chloride Threshold Values

These limits will give us the necessary information required to understand our results from the testing methods.

1.7 Need for Chloride

During cold weather, curing takes longer than usual time, increasing the cost and sometimes can reduce the standards of concrete resulting in an inferior product. In order to avoid this, accelerators (chemical admixture) are added to a concrete batch either immediately before or during mixing. Accelerators help the concrete to set

faster by increasing the rate of hydration. Early-strength concrete is designed to hydrate faster, often by increased use of accelerators in the mix. They also support early removal of forms, early finishing of concrete surface and early loading. Though chlorides have little to no effect on hardened concrete, they increase the risk of reinforcement corrosion. When concrete is properly cured, it increases strength and lowers the permeability and avoids cracking in dry surfaces. It is also essential to avoid freezing or overheating of the concrete due to exothermic setting of the cement. Improper curing can result in scaling, poor abrasion resistance, reduced strength and cracking.

1.8 Significance of Chloride in Concrete

Calcium chloride accelerates the cement hydration and reduces set time by nearly two thirds. Regardless of the mix design, it improves workability as less water is required to achieve the desired slump. It also improves strength of air-entrained concrete as calcium chloride compensates for the reduction in strength with a higher cement ratio. It also reduces bleeding due to the early accelerated stiffening. It is also responsible for the increase in the heat of hydration, flexural strength at 7 days and volume by 30 percent, 10 percent and 15 percent respectively and the decrease in tensile strength and flexural strength at 28 days by 15 percent.

When exposed for longer periods, concrete slowly carbonates and destroys the hydrogen atoms in concrete. Generally, the number of hydrogen atoms present in the Portland cement prevents corrosion of steel unless large amount of chlorides are present. When the base concentration is low, water and oxygen penetrate up to the

level of the steel. Sometimes, it leads to differential chloride content in the reinforced concrete structure.

1.9 Effect of Chloride in Concrete

Damage to concrete can be a result of many processes like the corrosion of reinforcement bars, expansion of aggregates, fire, freezing of water, bacterial corrosion and physical and chemical damage. In many parts of the world, concrete structures deteriorate rapidly due to chloride attack. The steel embedded in concrete develops a protective layer on its surface. This layer contains y-Fe703 adhering tightly to the steel which makes the steel remains intact. However, the chlorine ions present in the concrete destroys this layer, which, combined with water and oxygen leads to corrosion.

1.9.1 Spalling

This is the only effect of chloride taken into consideration in this study. Spalling (Figure 4) is the process of water entering concrete, brick or natural stone. As a result, the surface peels, pops out, or flakes off. It can eventually lead to the destruction of the structure. Spalling mainly occurs due to improper curing or hardening of concrete. It can also occur when the surface is subjected to exposed to higher concentration of salt (sodium chloride) resulting in oxidation and eventual rusting of reinforcing steel. As chloride ions reach steel, rust forms and can expand 10-15 times in volume causing cracking and spalling. (Figure 3)

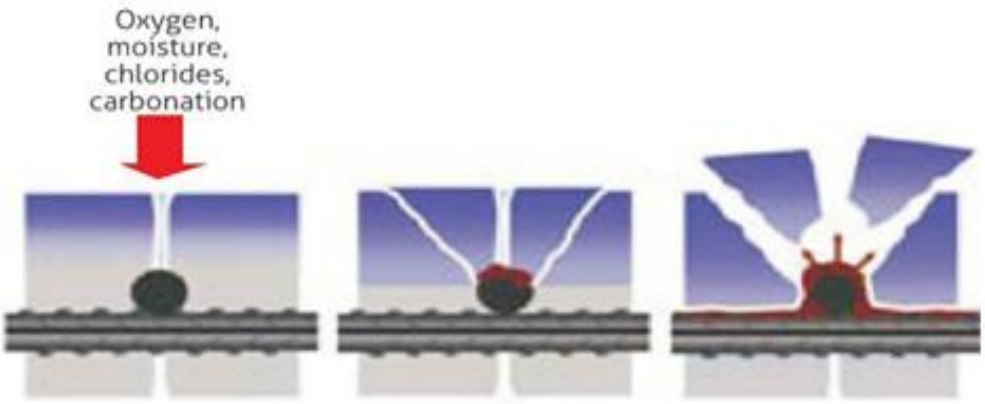

Figure 3: Expansion of Steel

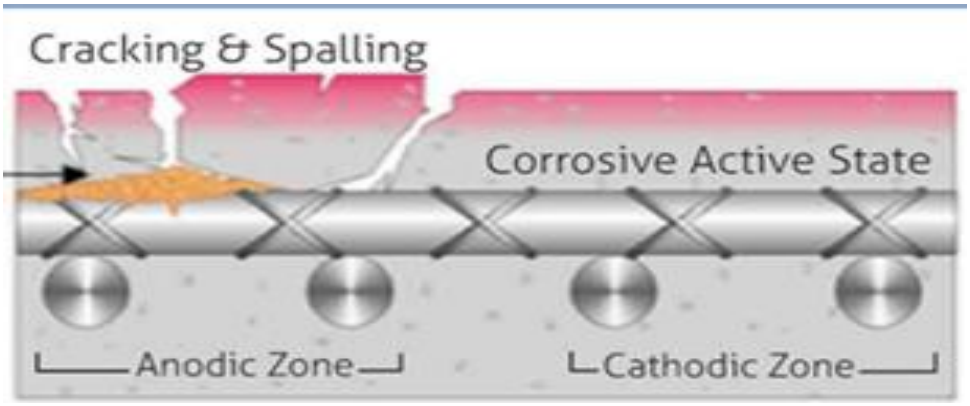

Figure 4: Spalling

Sometimes, alkalis in the concrete mix with the carbon dioxide in air forming cracks and admitting water. It can also occur due to changes in the weather conditions. Spalling is more likely in brick foundation and areas with high salt content. This can be rectified by replacing the bricks or by tuck-pointing.

1.10 Outline of the Thesis

This thesis consists of the following chapters:

- Chapter 1 is an introduction to the basis of this research and includes the background of the issue as well as the objective.

- Chapter 2 consists of the literature review relevant to this research and discusses about the work published over the years.
- Chapter 3 gives an overview of the testing methods currently available to measure the chloride ion penetration in concrete.
- Chapter 4 provides details about the work plan, sample requirements, mix design, the materials and their quantities.
- Chapter 5 focuses on the non destructive testing method using the Prompt Gamma-ray Activation Analysis. This chapter discuss in detail about the significance of PGAA, the experimental approach and the test data.
- Chapter 6 focuses on the destructive method and discusses the experimental approach and data of C1152 analysis and PGAA.
- Chapter 7 evaluates the test results and compares the two methods.
- Chapter 8 provides a summary of the study.

CHAPTER 2: LITERATURE REVIEW

2.1 Chloride Ion Penetration in Stressed Concrete

Li Guoping, Hu Fangjian and Wu Yongxian (2011) were one of the first to study the effect of stress due to chloride resistance of concrete. In their paper, they performed tests on the stressed specimens exposed to salt solution immersion and the chloride contents in uncracked concrete specimens were analyzed for different water-cement ratios, states and levels of stress, and environmental conditions. They deduced that the chloride ion presence is higher in stressed concrete when compared to unstressed concrete. The results showed that the resistance of concrete to chloride ion penetration can be improved by reducing the water-cement ratio.

2.2 Carbonation and Chloride-Induced Corrosion in RC Structures

In 2014, Yihui Zhou, B. Gencturk, Kaspar Willam and Arezou Attar studied about both carbonation-induced and chloride-induced corrosion that widely prevail in the construction industry in the paper 'Carbonation-Induced and Chloride-Induced Corrosion in Reinforced Concrete Structures'. Equation 4 explains the process of carbonation of concrete through series of reactions:

$$Ca(OH)_2 \rightarrow Ca^{2+}(aq) + 2OH^-(aq)$$

$$Ca^{2+}(aq) + 2OH^-(aq) + CO_2 \rightarrow CaCO_3 + H_2$$

$$3CaO \cdot 2SiO_2 \cdot 3H_2O + 3CO_2 \rightarrow 3CaCO_3 \cdot 2SiO_2 \cdot 3H_2O$$

$$3CaO \cdot SiO_2 + \mu H_2O + 3CO_2 \rightarrow 3CaCO_3 + SiO_2 \cdot \mu H_2O$$

$$2CaO \cdot SiO_2 + \mu H_2O + 3CO_2 \rightarrow 2CaCO_3 + SiO_2 \cdot \mu H_2O$$

Equation 4: Carbonation Process

Similarly, the process of chloride-induced corrosion was described in Equation 5

$$Fe^{2+} + 2Cl^{-} \rightarrow FeCl_2$$

$$Fe \rightarrow Fe^{2+} + 2e^{-}$$

$$O_2 + 2H_2O + 4e^{-} \rightarrow 4OH^{-}$$

$$Fe^{2+} + 2OH^{-} \rightarrow Fe(OH)_2$$

$$2Fe(OH)_2 + 12O_2 + H_2O \rightarrow 2Fe(OH)_3 \rightarrow Fe_2O_3 \cdot 3H_2O$$

Equation 5: Chloride Induced Corrosion

It was found that $CaCl_2$ is more corrosive in the concrete mixture compared to NaCl. As the chloride concentration increased, corrosion potential also increased resulting in deterioration of rebar area, ultimate strength, ultimate strain, and yield strength. In conclusion, corrosion causes cracking and spalling due to the expansive products present at the interface between concrete and rebar. It is also responsible for reducing the cross-sectional area of steel, risking the safety and serviceability of the structures.

2.3 Tests and Criteria for Concrete Resistant to Chloride Ion Penetration

This paper (2016), written by Karthik H. Obla, Colin L. Lobo, and Haejin Kim, focused on developing performance criteria to resist chloride ion penetration of concrete. Specimens were subjected to either chloride-immersion or periodic wetting and drying exposure in chloride solution. The research compared the results of chloride diffusion coefficients between ASTM C1556 and rapid index test methods including rapid chloride permeability, rapid migration, conductivity, absorption, and initial and secondary sorptivity. They observed that the Rapid Chloride Permeability Test (RCPT) was the best index test method in selecting mixtures based on their chloride penetrability for specimens in saturated and cyclic wet/dry conditions

relative to the apparent chloride diffusion coefficient of the mixtures. But, this method was not suitable for mix design with high water-cement ratio.

2.4 Diffusion Behavior of Chloride Ions in Concrete

In the paper by Tiewei Zhang and Odd E.Gjørv (1996), an analysis on the diffusion behavior of chloride ions in concrete is presented. They found that the effect of ionic interaction reduced the chemical potential of diffusion when electrolytic aqueous solution is used. This is due to the lagging of cations caused by different drift velocities of chloride ions. They also noticed that the electrical double layer forming on the solid surface and the chemical binding interferes with the transport of the chloride ions.

2.5 Evaluating Effect of Chloride Attack and Concrete Cover

In 2013, Sanjeev Kumar Verma, Sudhir Singh Bhadauria and Saleem Akhtar discussed in the paper 'Evaluating effect of chloride attack and concrete cover on the probability of corrosion' that a significant reason for corrosion of reinforced concrete structures is chloride ion penetration. According to the paper, chlorination is a major process governing the initiation and advancement of the injurious corrosion of steel bars. This article reviews about several chlorination studies and their results evaluating the effect of chloride on concrete including corrosion, compressive strength and concrete cover at rebar depth.

2.6 Probabilistic Model for the Chloride-Induced Corrosion

In the paper 'Probabilistic model for the chloride-induced corrosion service life of bridge decks', Trevor J. Kirkpatrick, Richard E. Weyers, Christine M. Anderson-

Cook, Michael M. Sprinkel (2002) have created a statistical model determining the time taken for the first repair and its subsequent rehabilitation of concrete bridge decks that are exposed to chloride deicer salts. The model was developed considering the statistical factors affecting corrosion and was based on existing diffusion cracking model. This model is extremely useful as it can quickly incorporate the data collected for corrosion deterioration duration after corrosion initiation. This paper was based on the information of surface chloride concentration, apparent diffusion coefficient and clear cover depth from 10 bridge decks in Virginia. The authors considered several ranges of chloride corrosion initiation and developed the simple and parametric bootstrap techniques to predict time of first repair and rehabilitation. The research confirmed that the results from both methods agree substantially for all the decks investigated.

2.7 Analysis of Total Chloride Content in Concrete

Saleh A. Al-Saleh (2015) presents an analysis of the total chloride content in concrete. This analysis was based on an experimental investigation of chloride quantity in cement, aggregates, mixing water. The author referred to the maximal total chloride limits for concrete based on British Standards to compare for the ingredients required for the mix. The results obtained suggested that the chloride content in mixing water has small to moderate effect upon the chloride content of concrete up to 0.4.

2.8 Chloride Penetration under Marine Atmospheric Environment

The paper 'Chloride penetration in concrete under marine atmospheric environment – analysis of the influencing factors' by Hongfei Zhang, Weiping Zhang, Xianglin Gu, Xianyu Jin & Nanguo Jin (2016) talks about the marine atmospheric exposure conditions provide a severe environment for reinforced concrete structures, mainly due to the occurrence of chloride-induced reinforcement corrosion. This procedure was influenced by many parameters related to the concrete properties and to the environmental condition. The aim of this study was to quantify the influence of different exposure conditions and its effect on the durability of concrete, measured by the chloride ingress in concrete. In this paper, cubic concrete specimens with 150-mm edge, different types of cementitious material and different strengths, were arranged on a structure, which exposed them to a natural marine atmospheric environment. When both relative humidity (RH) and temperature were monitored, it was observed that the relative humidity at the surface and temperature of the concrete were much different from that of the air. This was attributed to the fact that the diffusion coefficient and surface chloride concentration were time and location dependent. In addition, they were also influenced by the temperature, relative humidity and concrete strength. In case of long-term chloride penetration, it was also observed that incorrect results were possible when using constant diffusion coefficient and surface chloride concentration with the air RH and temperature.

2.9 Carbonation and Chloride Penetration in Marine Environment

The paper by A. Costa and J. Appleton (2001) details the findings of inspection of a series of 25-year-old concrete structures in a dockyard on the western coast of

Portugal, constructed with poor quality concrete. The structures were exposed to constant marine environment and it was evident that both carbonation and chloride penetration played a significant role in their deterioration. This was an anomaly as chloride penetration occurs more rapidly than carbon dioxide penetration in this environment. For this study, the authors considered a number of concrete slabs exposed to the marine environment for over a period of six years and their carbonation depth and chloride penetration were measured. It was found that when good quality concrete was used with an adequate concrete cover thickness to protect the reinforcement from the effect of chlorides, deterioration due to carbonation occurred only over a small part of the concrete cover layer. The authors deduced that carbonation rates were higher in the atmospheric zone, as the moisture content of the concrete was lowest. In contrast, the chloride penetration was lowest in the atmospheric zone. But based on the experimental results, the carbonation rate in medium and high quality concrete is found to be much lesser than the chloride penetration rate in any exposure zone of the marine environment. It was concluded that effect of carbonation on marine structures was of little significance when compared to the effect of chlorides.

2.10 Cold-Neutron Prompt Gamma-ray Activation Analysis

The paper ‘NGD cold-neutron prompt gamma-ray activation analysis spectrometer at NIST’ by Rick L. Paul, Dagistan NMN Sahin, Jeremy C. Cook, Christoph W. Brocker, Richard M. Lindstrom and Donna J. O'Kelly (2015) gives an insight into the cold neutron prompt gamma-ray activation analysis instrument designed for the cold neutron guide hall at the NIST Center for Neutron Research. When compared to the

PGAA instrument at NG7, this instrument could show up to a 10-fold increase in neutron flux with lower gamma-ray and neutron background. This instrument also yielded greater applicability, more sample space and better signal-to-noise ratio than the PGAA at NG7. In order to mitigate background and preserve the high neutron influence, the authors had used Monte Carlo based simulation software. They have also recommended some improvements to the instrument including optimization of neutron and gamma-ray shielding, improvement in sample space, installation of permanent evacuable neutron flight tubes, automatic sample changer, automated scanning stages for compositional mapping of samples, additional detectors for performing coincidence measurements and atmosphere/temperature controlled sample chambers for studying in situ reactions.

CHAPTER 3: TESTING METHODS

3.1.Objective

The primary objective of this study was to compare the results between destructive and non destructive testing of chlorine in concrete. The aim is to provide a viable alternate to the existing destructive methods. This chapter gives an overview of the existing testing methods but focuses only on two methods for comparison- C1152 and PGAA.

3.2.PGAA

Prompt Gamma-ray Activation Analysis (PGAA) is a nondestructive elemental analysis widely used in determining the presence and amount of many elements ranging in size from micrograms to many grams. As it is a non-destructive method, the chemical form and shape of the sample are relatively unimportant. Typical measurements can be taken from few minutes to several hours per sample. One of the main concerns is radioactivity but in this method, the sample will not acquire considerable long-term radioactivity. So, the sample may be removed from the facility and used for other purposes after the radioactivity level reduces below the permissible limits.

The cold neutron instrument is designed to minimize background and maximize the neutron flux. The instrument is shielded in such a way that they avoid generating a background of capture and decay gamma rays. Li-6 is used in collimators and absorbers whereas antimony-free lead is used for gamma shielding. The purpose of the cold neutron beam is to maximize the neutron flux. This is possible by passing

cold liquid hydrogen at 20.28K (ideal temperature for hydrogen to be in liquid state without boiling). Due to this technical advancement, the instrument can detect hydrogen even less than 1 microgram and provides sensitivity up to 20 times better than any thermal beam in existence. The specimen will not acquire considerable long-term radioactivity and hence it is not a factor to be concerned.

3.3.C1152

C1152 is the Standard Test Method for Acid-Soluble Chloride in Mortar and Concrete. This test is used to analyze the acid-soluble chloride present in the hydraulic-cement mortar or concrete. The amount of acid-soluble chloride in the hydraulic cement systems is equal to the total amount of chloride in the system or equivalent to total chloride in the system. After a period of exposure, acid-insoluble chloride can ionize and become acid-soluble or water-soluble due to some organic substances in the mortar or concrete. For instance, sulfides interfere with the determination of chloride content. Additives such as blast-furnace slag, aggregate and cement contain concentrations of sulphur, causing interference and erroneous results. In order to overcome this interference, the samples are generally treated with hydrogen peroxide. This method is also used to detect non corrosion causing chlorides present in the aggregates.

3.4.C1556

C1556 is the Standard Test Method for Determining the Apparent Chloride Diffusion Coefficient of Cementitious Mixtures by Bulk Diffusion. This method is used to determine the apparent chloride diffusion using laboratory techniques. Two samples

of cementitious mixture are required. One specimen (test sample) is obtained prior exposure to chloride ion and the other one after the exposure. The initial chloride-ion content specimen is crushed and the initial acid-soluble chloride-ion is measured. Except for the finished surface, the test specimen is sealed on all sides with a suitable barrier coating. The sealed specimen is saturated in calcium hydroxide solution, rinsed and placed in sodium chloride solution. After specific exposure time, the test specimen is removed from the sodium chloride solution. The thin layers parallel to the exposed surface of the specimen are scraped and the acid-soluble chloride content of each layer is determined. The apparent chloride diffusion coefficient and the chloride-ion concentration of the exposed surface are calculated based on the initial chloride-ion content.

3.5.NT Build 492 Test

The NT (Non-Steady State Migration Test) Build 492 (Nord Test) was initially proposed by Tang and Nilsson in 1991. It is also known as the Rapid Chloride Migration Test (RMT). In this method, the depth of chloride penetration is measured to determine the chloride migration coefficient under non-steady state. When the specimen is subjected to external electrical voltage, the chloride ions are forced to move into the concrete. Due to electro-potential difference, the chloride ions migrate from the 10% NaCl solution to the 0.3 M NaOH solution, through the concrete. The specimen is then divided into two and sprayed with AgNO3, to measure the chloride penetration. AgNO3 is preferred as it is generally used as an indicator for chlorides. Now, the chloride migration coefficient can be calculated based on the value obtained by this measurement. This is a very simple and reliable method and can be used for

different types of concrete and also for specimens cast in a laboratory or drilled from field. Since the charge passed affects all the ions and increases the temperature, this test is criticized by scientist. But due to its quick results, this test is widely in use.

3.6.ASTM C1202

The Rapid Chloride Permeability Test (RCPT) or the Coulomb Test was first developed by Whiting (1981). It is also referred to as the ASTM C1202 and AASHTO T277 test. The test procedure is the same as that in the NT Build 492 test, except that the saturation medium is different ($Ca(OH)_2$ in the NT Build 492 test and water in Coulomb Test) and electric charge passed over a period of 6 hours. The setup consists of 3% NaCl (cathode) solution on one side and 0.3 N NaOH (anode) solution on the other. The amount of charge passing through the specimen is determined by plotting the current as a function of time. After passing the charge for 6 hours, the total charge is determined in Coulombs by calculating the area under the plot of current versus time. In the anode cell, the chloride ion concentration conducted is measured using an ion chromatograph at pre-determined intervals.

3.7.Problem Statement

The most commonly used method to acid-soluble chloride in concrete is ASTM C1152. However, it has the following disadvantages:

- Destructive Analysis
- Time Consuming
- Costly and complex to subject building structures and large non-building structures

- Not convenient to apply to parts of a structure
- Cannot measure cumulative change over a period of time
- Cannot be employed on structures actually used in service

Hence, this research aims to find a viable alternate (PGAA) to measure the chloride content in concrete.

CHAPTER 4: GROUNDWORK

4.1 Work Plan

In this study, samples will be prepared in batches to be tested in both destructive and non destructive methods. One sample of each batch is to be considered as the intact sample. These samples will be used for the non destructive testing in PGAA with a slit collimator to measure the chlorides. The remaining samples are to be powdered and tested in C1152 and PGAA for direct comparison with C-1152. The PGAA method will be conducted at the NCNR facility in NIST whereas the C1152 analysis will be conducted at NRMCA. The results from both the destructive and non destructive methods will be compared to comprehend the benefit of PGAA.

The experimental program requires two groups of concrete samples in four batches. Three batches had chloride added to the mix - 0.2%, 0.1%, 0.01% by weight of cement whereas the fourth batch had no additional chloride added (Control batch). The selection of these specific levels of chloride is to evaluate the performance of these two methods at the levels corresponding to the threshold for corrosion, 0.1-0.2% by weight of cement.

The work flow for this study is described in Figure 5.

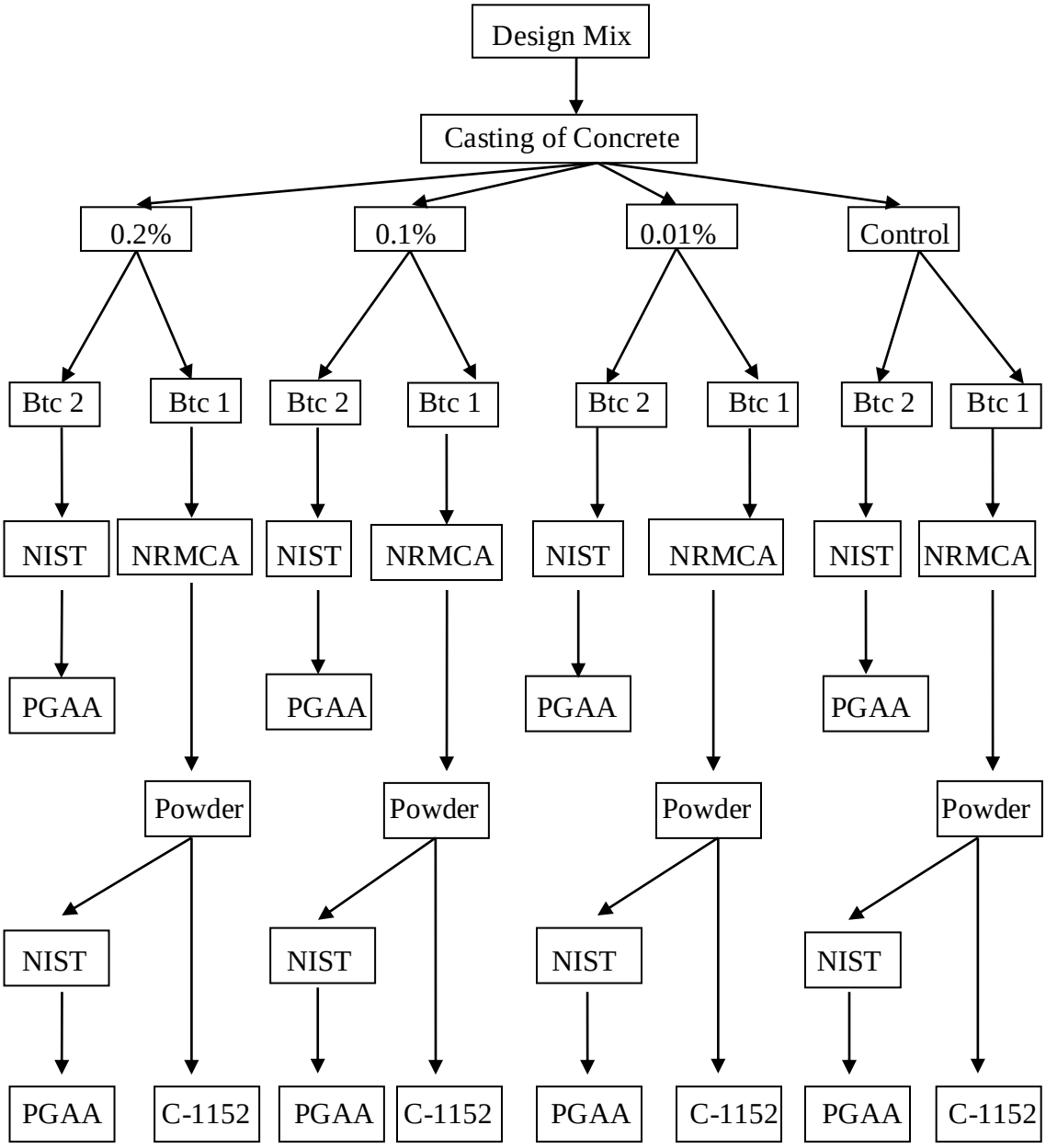

Figure 5: Work Plan

Btc – Batch

4.2 Sample Requirements

The number of samples and positions required for each analysis is given in Table 1 and Table 2. It is important to note that the powder sample mentioned in both PGAA and C1152 is from the same batch (i.e. the powder obtained from one sample is divided and tested in both analysis).

Table 1: Number of Samples for PGAA

Batch	**Control**	**0.01%**	**0.10%**	**0.20%**	**Total**
Powder	1	1	1	1	4
Cylinder *	1	1	1	1	4
Total	2	2	2	2	8

* 3 positions on each

Table 2: Number of Samples for C1152

Batch	**Control**	**0.01%**	**0.10%**	**0.20%**	**Total**
Powder	1	1	1	1	4
Cylinder	0	0	0	0	0
Total	1	1	1	1	4

From the above information, it is evident that C1152 is used only for the destructive testing whereas PGAA is used in destructive and non destructive modes.

4.3 Sample Dimensions

All the samples were prepared with consistent dimensions as the aim was to compare the two methods in similar setting. The number of samples required, their overall dimensions, mass and volume are given in Table 3.

Table 3: Sample Measurements

Diameter of the cylinder	6.35 cm
Height of the cylinder	5 cm
Volume of the cylinder	158.35 cm^3
Mass of the cylinder	0.38 kg (0.836 lbs)
No. of Batches	4
Samples per batch	2
Volume of each batch	316.69 cm^3
Mass of each batch	0.76 kg (1.672 lbs)

4.4 Design Mix

The design mix is based on the sample dimensions mentioned above. Design mix software (Figure 6) was used and the following conditions were considered.

- Characteristic Compressive Strength: 4000 psi
- Density of Concrete : 2400 kg / m^3
- Maximum size of the coarse aggregate: 10 mm
- Degree of workability: 0.92
- Type of Exposure: Mild
- Cement Used: Portland Cement- Type I
- Specific Gravity of Cement: 3.15
- Slump: 75-100 mm
- Water-Cement Ratio: 0.4

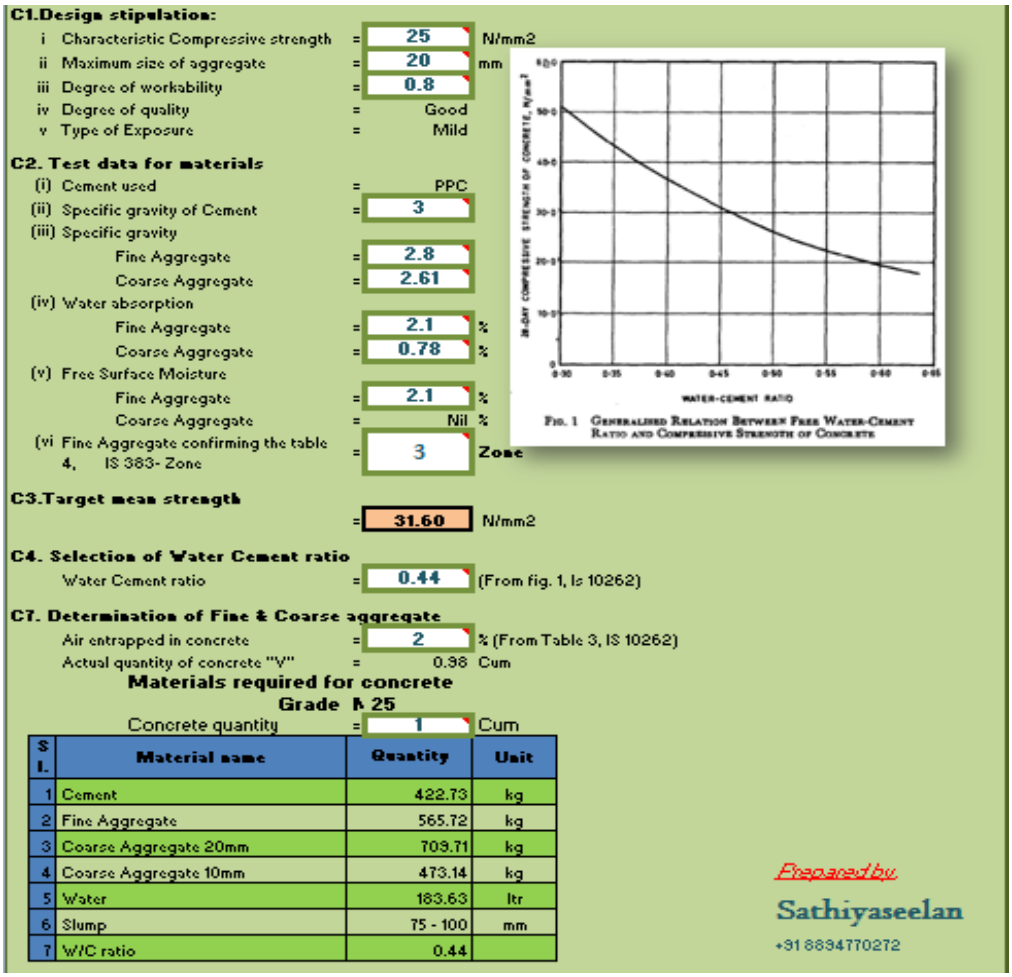

C1.Design stipulation:

i	Characteristic Compressive strength	25	N/mm2
ii	Maximum size of aggregate	20	mm
iii	Degree of workability	0.8	
iv	Degree of quality	Good	
v	Type of Exposure	Mild	

C2. Test data for materials

(i)	Cement used	PPC	
(ii)	Specific gravity of Cement	3	
(iii)	Specific gravity		
	Fine Aggregate	2.8	
	Coarse Aggregate	2.61	
(iv)	Water absorption		
	Fine Aggregate	2.1	%
	Coarse Aggregate	0.78	%
(v)	Free Surface Moisture		
	Fine Aggregate	2.1	%
	Coarse Aggregate	Nil	%
(vi	Fine Aggregate confirming the table 4, IS 383- Zone	3	Zone

FIG. 1 GENERALISED RELATION BETWEEN FREE WATER-CEMENT RATIO AND COMPRESSIVE STRENGTH OF CONCRETE

C3.Target mean strength

31.60 N/mm2

C4. Selection of Water Cement ratio

Water Cement ratio = 0.44 (From fig. 1, Is 10262)

C7. Determination of Fine & Coarse aggregate

Air entrapped in concrete = 2 % (From Table 3, IS 10262)

Actual quantity of concrete "V" = 0.98 Cum

Materials required for concrete

Grade M 25

Concrete quantity = 1 Cum

S I.	Material name	Quantity	Unit
1	Cement	422.73	kg
2	Fine Aggregate	565.72	kg
3	Coarse Aggregate 20mm	709.71	kg
4	Coarse Aggregate 10mm	473.14	kg
5	Water	183.63	ltr
6	Slump	75 - 100	mm
7	W/C ratio	0.44	

Prepared by

Sathiyaseelan

+91 8694770272

Figure 6: Design Mix

4.5 Raw Material Quantities

Although the quantities were specified using the design mix software, wastage was taken into consideration. Hence actual quantities used in the mix will be larger than the design quantities but the proportions will be the same. The raw materials used in the preparation of the concrete samples are from the following places:

- Coarse Aggregate – #7 Stone –Martin Marietta, Medford Quarry, New Windsor, MD
- Fine Aggregate – Rappahannock Farms, Fredericksburg, VA
- Cement – Lehigh Type I/II Union Bridge, MD

The quantities of raw materials actually used are compared against the target quantities specified by the mix design and are given in Table 4. The cylinders as cast are shown in Figure 7.

Table 4: Quantity of Raw Materials

Raw Material	**Target Quantity (lbs)**	**Actual Quantity (lbs)**
Cement	0.403	0.405
Fine Aggregate	0.086	0.087
Coarse Aggregate	1.026	1.028
Water	73	100

The quantities of CaCl2 added to each batch are presented in Table 5. This also has a column giving the actual Cl% values, which are roughly twice the target values. The difference is due to two issues with the design calculations. First, the Cl mass fraction in $CaCl_2$ used in the calculations was incorrectly given as 0.469 whereas the correct value is 0.639. Second, the mass of cement was assumed to be 0.563 lbs, but as shown in Table 4, this was actually 0.405 lbs. The discrepancy between the target and actual values of Cl% does not invalidate this research because the latter are still at the right order of magnitude. For consistency, the batches will continue to be identified by their target values.

Table 5: Percentage of Chloride added by weight of Cement

Target Cl % wt.cem.	**Target Quantity (lbs)**	**Actual Quantity (lbs)**	**Actual Cl % wt.cem.**
0.20%	0.0024	0.0024	0.380
0.10%	0.0012	0.0013	0.200
0.01%	0.00012	0.00013	0.0202

Figure 7: Cast Samples

CHAPTER 5: NON DESTRUCTIVE TESTING

PROMPT GAMMA-RAY ACTIVATION ANALYSIS

5.1 Aim

The objective is to perform a non destructive analysis of chloride penetration in concrete specimens. In order to understand the chloride penetration, it is essential to analyze the samples at varying depths. Hence, this research will consider three vertical positions on each sample – at 1 cm, 2.5 cm and 3.6 cm from the base of the concrete cylinder. The neutron beam will be focused on each position to study the chloride ingress.

5.2 Principle

Samples are irradiated by a beam of neutrons inducing elemental nuclei to capture neutrons (Figure 8). **The samples emit characteristic prompt gamma rays upon de-excitation which are measured with a gamma ray spectrometer**. Under a high resolution germanium detector, the gamma ray energies identify the neutron-capturing elements and the intensities of the peaks at these energies reveal their concentrations. The gamma ray production at a point within the target is given by the formula

$$\gamma_i = n\sigma_a^i f^i y_k^i \phi_{th}$$

where γ_i = gamma ray production rate, photons / s

n = number density of atoms of element

σ^i_a = neutron capture cross-section of i^{th} isotope

f^i = abundance of i^{th} isotope

y^i_k = yield of k^{th} gamma ray for i^{th} isotope

ϕ_{th} = thermal neutron flux, neutrons/cm^2· s

The product $\sigma_a^i f^i y_k^i$ is known as the partial cross section and it is a constant for a given isotope and gamma ray energy. The thermal neutron flux is known. Consequently the number density is the only unknown variable in the equation, and thus it can be calculated from the observed gamma ray signal.

The amount of analyte element is given by the ratio of count rate of the characteristic peak in the sample to the rate in a known mass of the appropriate elemental standard irradiated under the same conditions.

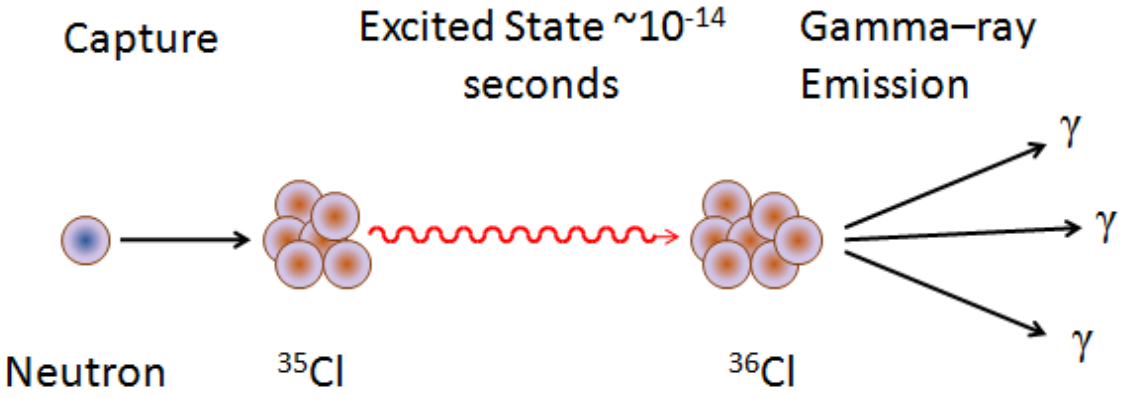

Figure 8: Prompt Gamma Neutron Activation

The capability of PGAA for detecting various elements is indicated in Table 6. This shows that for certain elements such as boron or cadmium the minimum level is as low was 10 parts per billion. Elements that are relevant for the problem of chlorides in concrete are highlighted. In particular, Cl can be detected down to 0.1 parts per million.

Table 6: Minimum Levels of Detection for NIST Cold Neutron PGAA

(24 hours irradiation)

Range (mg)	Elements
0.01 - 0.1	B, Cd, Sm, Gd
0.1 – 1	H, **Cl**, In, Nd
1 – 10	Na, S, K, Sc, Ti, V, Cr, Mn, Co, Ni, Cu, Ge, As, Se, Br, Mo, Ag
1 – 100	Mg, Al, **Si**, P, Ca, Fe, Zn, Ga, Rb, Sr, Y, Zr, Nb, Sb, Ba, La
100 – 1000	C, N, F, Sn, Pb

5.3 PGAA-NIST

The cold neutron PGAA instrument is located in the guide hall NGD 100 in the National Institute of Standards and Technology (NIST). This instrument is used to certify inorganic SRMs and to trace hydrogen and boron in materials.

The cold neutron PGAA station (Figure 9) consists of a sample chamber, a BGO (Bismuth germanium oxide) detector, High Purity Germanium (HPGe) detector, flight tubes and a shutter to control the neutron beam. These n-type Ge detectors have an efficiency of 41 % and resolution of 1.75 keV. The germanium detector is equipped with a transistor-reset preamplifier for high count rates and hence accounts for better sensitivity. The insides of the PGAA instrument consist of a neutron beam port to allow the neutron beam to enter the chamber.

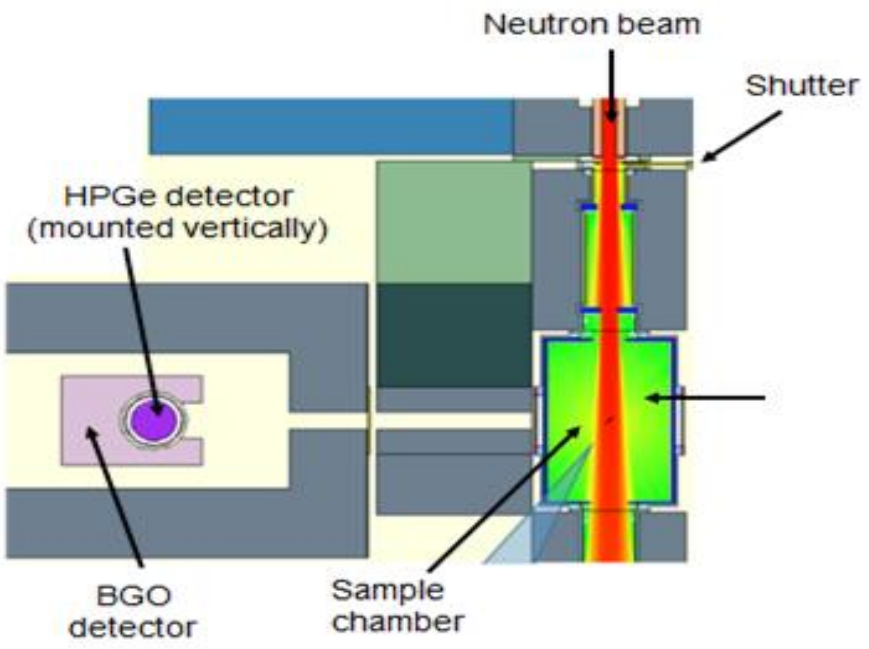

Figure 9: Cold Neutron PGAA Station, NCNR

Lead shielding is provided on all sides (Figure 10) with Li glass cover which acts as a permanent beam stop. The lead collimators are mounted in front of the detector and control the gamma-ray signal from the sample. In order to shield gamma ray background from scattered neutrons, the front of the lead collimators is covered by lithiated polymer whereas the rest is covered by thick cadmium.

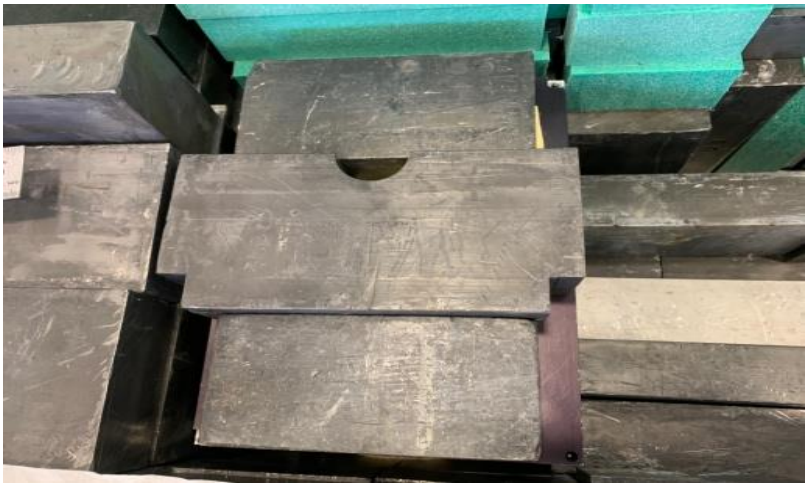

Figure 10: Sample Chamber with Lead Covering

The gamma rays have energies up to 11 MeV and the neutron flux has a thermal equivalent of 6.5 x 10^9 $cm^{-2}s^{-1}$. An extra shielding of lead bricks is provided between the beam and the sample chamber. This shielding protects the detector from gamma-ray background arising due to neutron capture in the flight tubes and chamber, the guide exit window and the vacuum chamber windows. The ^{35}Cl with 1951 keV is considered for this experiment.

5.4 Slit Collimation Setup

In the normal setup, the HPGe gamma ray detector views the sample through a 1" circular opening in the lead shielding surrounding it. However, to investigate the possibility of using PGAA to scan intact cylinders, a slit collimator was temporarily installed between the detector and the target. This consisted of two lead bricks separated by a 2 mm gap, as shown in the plan view in Figure 11. The combination of the neutron beam 2 cm width and the 1" aperture in the detector shield defined a rectangular detection volume in the sample 2 cm by 2.5 cm by 2 mm. Since the height of the collimator is fixed, the scanning of the sample was accomplished by mounting it on a lab jack who could be adjusted for elevation in Figure 12.

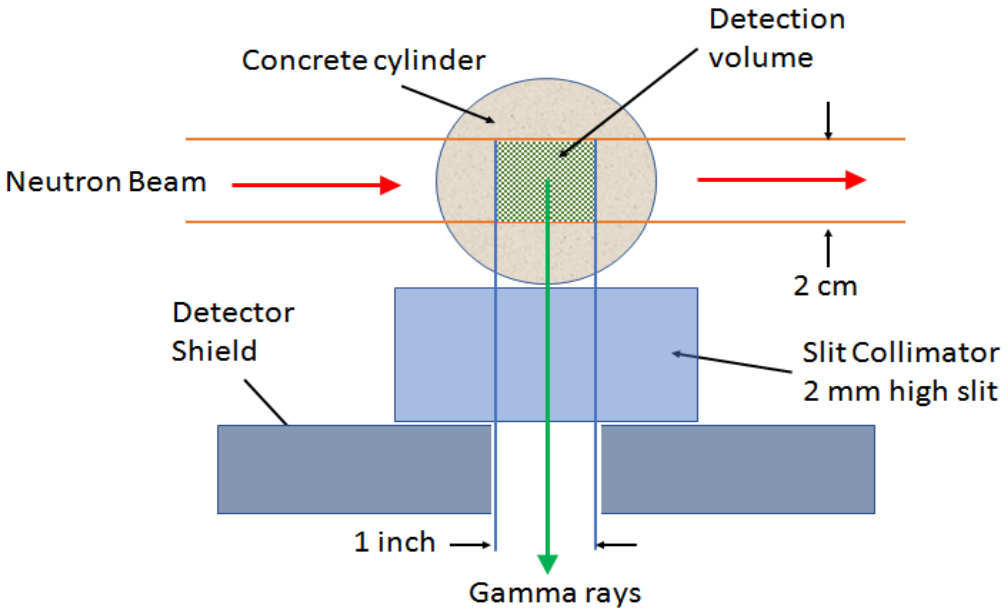

Figure 11: Plan view of the slit collimator setup.

The target-collimator and collimator-detector separation distances have been omitted for clarity.

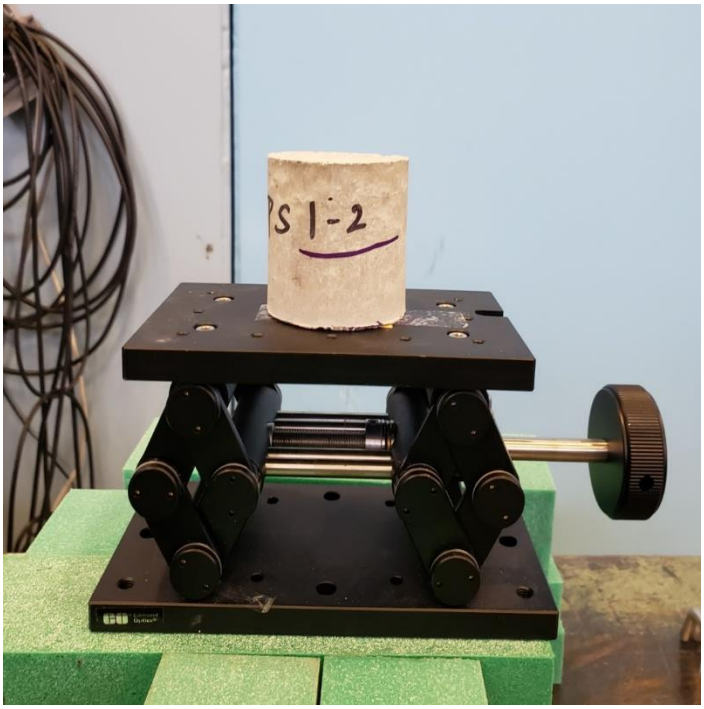

Figure 12: Concrete Cylinder on the lab jack

5.5 Procedure

- The sample is placed inside the sample chamber (Figure 13) on the lab jack, facing the collimator.
- Care must be taken when sealing the chamber with lead bricks.
- Once the set up is complete, the beam is switched on and analyzed for a fixed time, typically 2 hours.

Figure 13: Sample Chamber

- The statistics of the chlorine and silica peaks at gamma ray energies of 1951 keV and 1273 keV respectively are periodically checked.
- When the uncertainties of these values are below 5%, the analysis is stopped.
- A decay spectrum is then acquired for roughly 10 minutes to determine the residual radioactivity of the sample and to allow the reduction of the radiation level to safe levels for handling the sample.

5.6 PGAA Data Acquisition

During the PGAA counting, the data acquisition is controlled by The Genie 2000 software. This manages the Lynx electronic module which turns on and off the HPGe detector. The software also continuously displays the gamma spectrum being acquired. Finally, during the counting Genie 2000 can generate a report on various statistics about the peaks including centroid, background, area, count rate and uncertainty. Table 7 provides examples for the Cl 1951KeV and Si 1273 keV peaks and Figure 14 shows the ratio of Cl to Si for each sample.

Table 7: PGAA Data of Cylinders

Sample	% of Cl added by weight of cement	Position of the Beam (cm)	Area		Area of Cl / Area of Si	Area of Cl / Area of Si (without control)
			Cl 1951	Si 1273		
PS 1-2-1	0.2%	1	43212	23992	1.801	1.484
PS 1-2-2	0.2%	2.5	50327	26736	1.882	1.621
PS 1-2-3	0.2%	3.6	48132	28170	1.709	1.340
PS 2-2-1	0.1%	1	17601	17175	1.025	0.708
PS 2-2-2	0.1%	2.5	20338	18367	1.107	0.846
PS 2-2-3	0.1%	3.6	36650	31302	1.171	0.802
PS 3-2-1	0.01%	1	8928	24723	0.361	0.044
PS 3-2-2	0.01%	2.5	5538	16340	0.339	0.077
PS 3-2-3	0.01%	3.6	2744	6958	0.394	0.026
PS 4-2-1	Control	1	7773	24508	0.317	
PS 4-2-2	Control	2.5	7270	27824	0.261	
PS 4-2-3	Control	3.6	15870	43043	0.369	

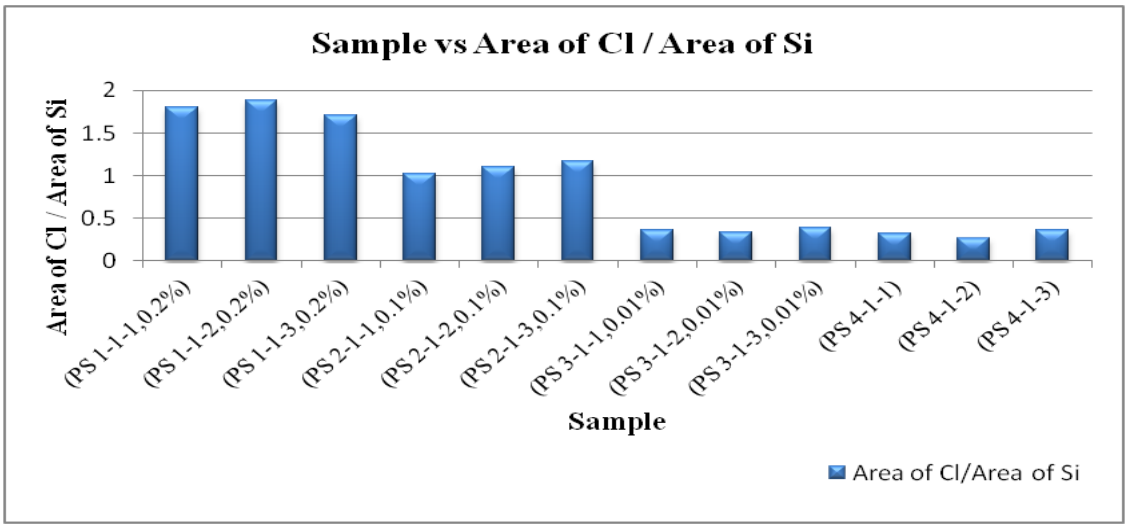

Figure 14: Sample vs. Cl/Si

The test was run until we reached an uncertainty level below 5%. This shows that we can have control over the accuracy of the result making this method a reliable one. The uncertainties of Cl & Si for each sample are listed in Table 8.

Table 8: Uncertainty in NDT-PGAA

Sample	% of Cl added by weight of cement	Position of the Beam (cm)	Uncertainty %	
			Cl 1951	Si 1273
PS 1-2-1	0.2	1	1	1.4
PS 1-2-2	0.2	2.5	0.9	1.4
PS 1-2-3	0.2	3.6	1	1.2
PS 2-2-1	0.1	1	2.1	1.7
PS 2-2-2	0.1	2.5	1.8	1.6
PS 2-2-3	0.1	3.6	1.3	1.3
PS 3-2-1	0.01	1	4.4	1.3
PS 3-2-2	0.01	2.5	6.2	1.8
PS 3-2-3	0.01	3.6	8.1	2.9
PS 4-2-1	Control	1	5.5	1.5
PS 4-2-2	Control	2.5	5.7	1.4
PS 4-2-3	Control	3.6	2.8	1

5.7 PeakEasy Software

PeakEasy software is used for the detailed analysis of the gamma-ray spectrum after counting. PeakEasy allows loading and displaying of spectra data files from over 120 different file formats. The graphical interface of the PeakEasy Software is shown in Figure 15 which displays the analysis of the Cl 1951 keV peak.

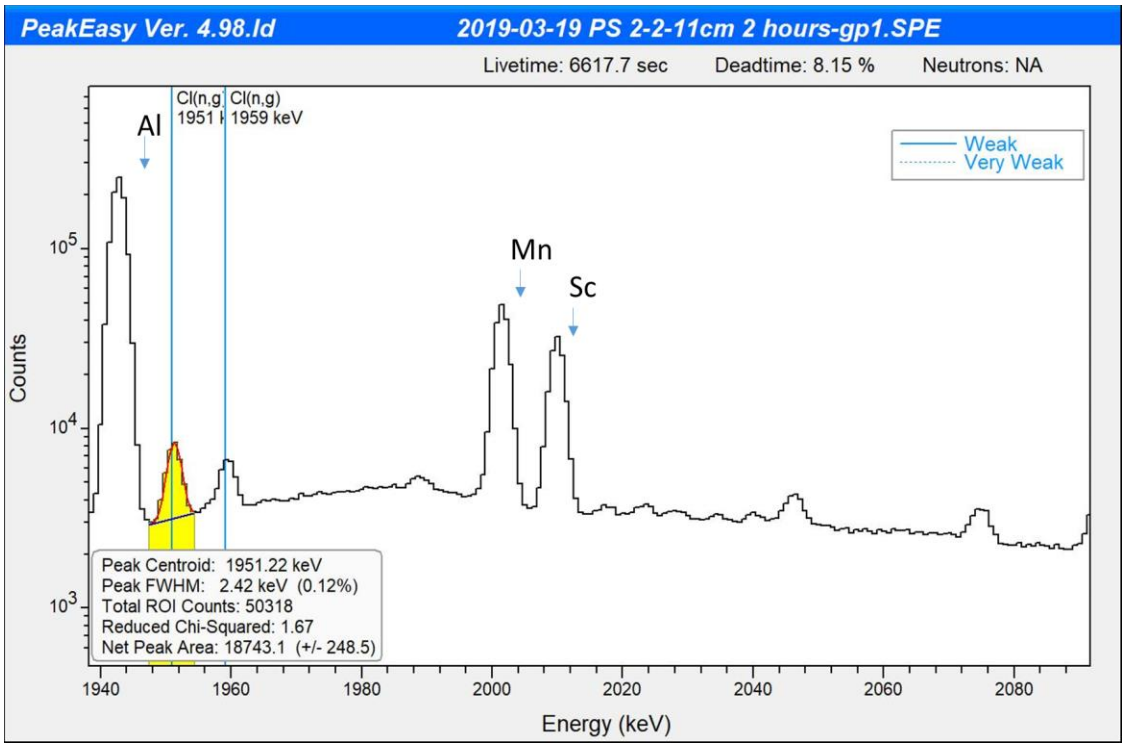

Figure 15: PeakEasy Interface

The data collected from the PGA analysis is stored according to the chlorine concentration, position of the beam on the sample and the raw materials. These files are fed into the PeakEasy software to find the peak intensities of Chlorine-isotope 36, and Silica-isotope 29. The result of each sample processed by the software is given in Appendix from Table 21 to Table 32. The chloride concentration (%) of all the samples is found by the ratio of the mass of Cl at 1951 keV and the mass of the

cylinder and presented in Table 9 and Figure 16. The concentration of chlorides in the sample is very small and this result confirms that the cold neutron PGAA can detect amounts of chloride concentration at the corrosion threshold.

Table 9: Cl content (%) in Cylinders

Sample	% of Cl added by weight of cement	Position of the Beam (cm)	Cl %
PS 1-1-1	0.2	1	0.00192
PS 1-1-2	0.2	2.5	0.0023
PS 1-1-3	0.2	3.6	0.00216
PS 2-1-1	0.1	1	0.00079
PS 2-1-2	0.1	2.5	0.00091
PS 2-1-3	0.1	3.6	0.00167
PS 3-1-1	0.01	1	0.00044
PS 3-1-2	0.01	2.5	0.00025
PS 3-1-3	0.01	3.6	0.00011
PS 4-1-1	Control	1	0.00034
PS 4-1-2	Control	2.5	0.00023
PS 4-1-3	Control	3.6	0.00053

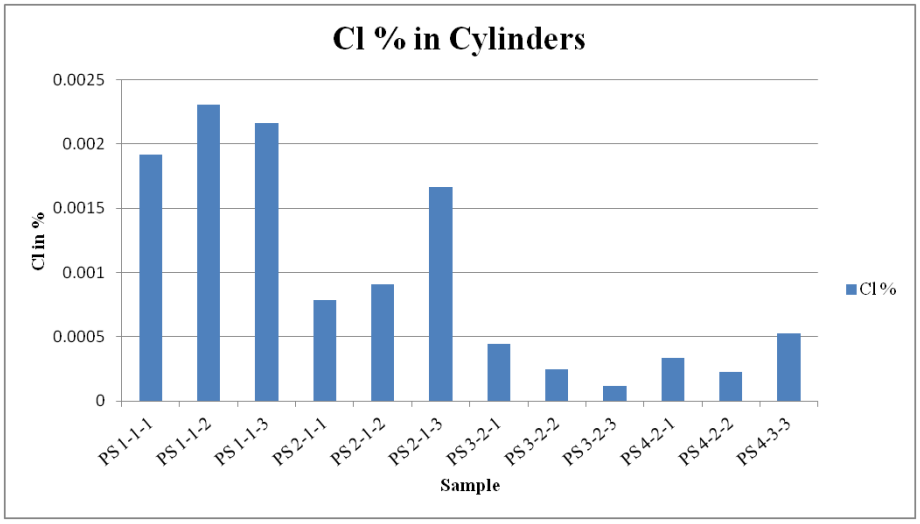

Figure 16: Cl content (%) in Cylinders

CHAPTER 6: POWDERED TESTING

SECTION A: C1152

6.1.Overview

The second phase of this project is the testing of the samples in the form of powdered concrete using two methods- The ASTM C-1152 (Standard Test Method for Acid-Soluble Chloride in Mortar and Concrete) and Prompt Gamma-ray Activation Analysis.

6.2.Apparatus Required

- Rotary Impact Drill
- Sample Containers
- Sample Processing Apparatus
- Stirrer
- Chloride Ion Selective Electrode
- 850-µm (No. 20) Sieve

6.3.Reagents Required

- Nitric Acid
- Hydrogen Peroxide
- Distilled Water
- Sodium Chloride, Standard Solution (0.05 M NaCl)
- Silver Nitrate, Standard Solution (0.05 M ($AgNO_3$))

6.4.Sample Required

Three positions are marked in the sample (at 1 cm, 2.5 cm and 3.6 cm). Each cylinder block is powdered at the marked positions using the rotary impact drill (Figure 17). No lubricant is used when drilling and care is taken to prevent sample contamination. It is better to obtain at least 20 g of powdered material for each position. This powdered sample will be used in both C1152 and PGAA. The pulverized sample is passed through 850-µm (No. 20) sieve to obtain the finer powder.

Figure 17: Rotary Drill in NRMCA

6.5.Procedure

- Approximately 2 g of sample is taken and dispersed with 75 ml of water.
- About 15 ml of dilute nitric acid and 3 ml of hydrogen peroxide are added and stirred to break the lumps.

- The beaker is covered and allowed to stand for 1-2 minutes.
- The beaker is boiled for few seconds at high temperature
- The solution is then filtered by suction using Buchner funnel and flask.
- The electrodes are immersed in a small portion (sub sample) of the filtrate and placed below the burette containing 0.05N $AgNO_3$ solution. (Figure 18)
- The whole setup is placed on a magnetic stirrer for gentle stirring.
- As the equivalence point is approached, the equal additions of silver nitrate solution will cause larger and larger changes in the milli-voltmeter readings.
- After this point, the change per increment will decrease.
- The volume of silver nitrate titrated will be provided by the ProoveIt software.

Figure 18: C1152 Testing Apparatus

6.6.Chloride Calculation

The Cl^+ ion in the sample solution is precipitated with the Ag^- ion by the reaction:

$$Ag^+ + Cl^- \rightarrow AgCl\downarrow \quad (1)$$

The mass of the AgCl precipitate is calculated from the volume of $AgNO_3$ solution used by the equation:

$$m_{cl} = \frac{f_{cl} r M_{AgNO_3} N}{1000} V \quad (2)$$

where m_{cl} = mass of Cl in precipitate

V = volume of AgNO3 solution used for sample titration in ml

N = normality of AgNO3 solution

M_{AgNO3} = molecular weight of $AgNO_3$ = 169.87 g/mol

r = molecular weight of AgCl / molecular weight of $AgNO_3$ = 143.32/169.87 = 0.854

F_{cl} = mass fraction of Cl in AgCl = 35.453/143.32 = 0.2473

Note that normality is used here in accordance with the language of ASTM C 1152. However, its use is currently discouraged in the field of chemistry and molarity is recommended instead. In this case, the molarity and the normality is the same. Inserting the numerical values of the constants in Eqn(2) gives:

$$m_{cl} = 0.03545NV \quad (3)$$

Finally, the m_{cl} is converted into the chloride percentage by weight of concrete by dividing by the mass, w, of the sample:

$$Cl\% = \frac{100 * m_{Cl}}{w} \quad (4)$$

The results of the C 1152 measurements are summarized in

Table 10. For the control sample the Cl level was below the minimum level of detection. Therefore a volume of solution with known Cl^- concentration was added,

and the titration was repeated. However, subtracting the additional Cl^- from the measured values gave negative numbers, due to the very low concentrations involved and the uncertainties of the method.

Table 10: Cl content (%) in Powdered Samples from C1152

Sample ID	Depth (mm)	Test Powder (g)	Filtrate (g)	Sub Sample (g)	AgNO3 (ml)	TW (g)	Chloride (%)
PS 1-1	10	2.0456	91.0	14.1	0.3715	0.317	0.042
PS 1-1	25	2.0503	96.0	14	0.3362	0.299	0.040
PS 1-1	36	2.0103	96.9	14	0.2697	0.290	0.033
PS 2-1	10	2.031	91.6	14.1	0.2095	0.313	0.024
PS 2-1	25	2.0343	87.9	14.1	0.2343	0.326	0.025
PS 2-1	36	2.0918	89.6	14	0.2313	0.327	0.025
PS 3-1	10	2.0131	82.0	14.4	0.1745	0.354	0.017
PS 3-1	25	2.0212	87.3	13.9	0.1659	0.322	0.0183
PS 3-1	36	2.0968	90.1	13.7	0.1877	0.319	0.0209
PS 4-1	10	2.0105	84.1	15.1	1.7500	0.361	-0.0143
PS 4-1	25	2.0878	90.0	14.1	1.9850	0.327	-0.0122
PS 4-1	36	2.0195	77.2	14.9	1.9832	0.390	-0.0128

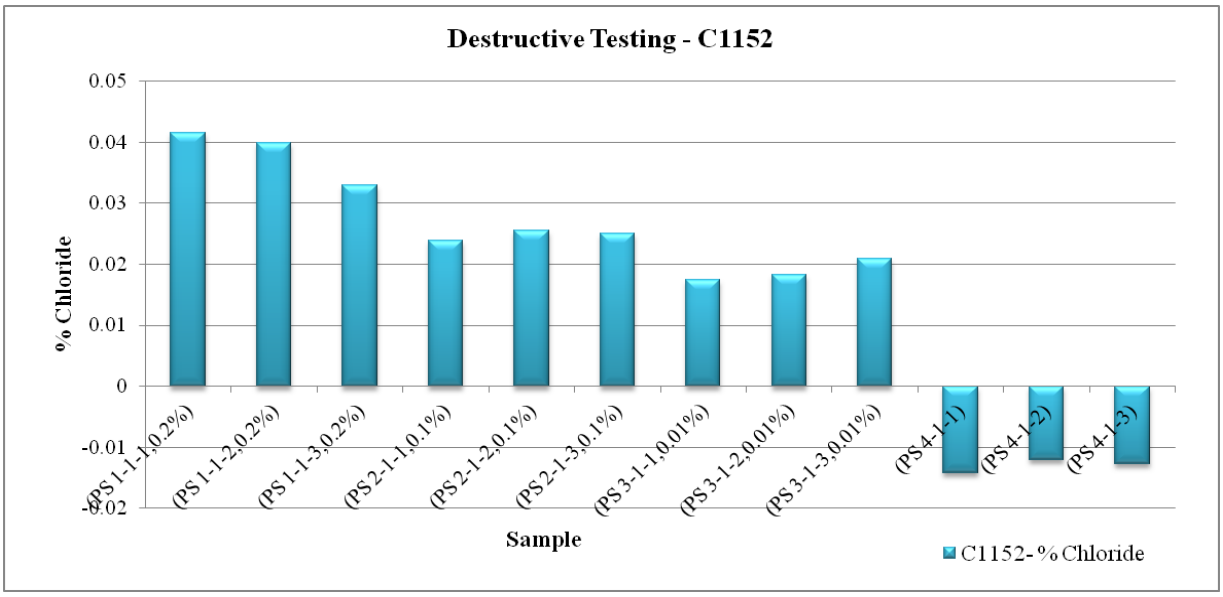

Figure 19: Cl content (%) in Powdered Samples from C1152

Figure 19 shows a graphical representation of the Cl levels in the powder samples.

SECTION B: PGAA

6.7.Sample Selection

A portion of the powder samples prepared for the C1152 test were reserved for analysis by PGAA. It was observed during the analysis of the intact samples that, in the Cl signal from the calcium chloride added to the batches, the raw materials (cement, coarse aggregate and sand) might contain chloride ions which would make a substantial difference in the test results. Hence, it is essential to analyze the raw materials for their chlorine contribution. The cement powder was compressed into pellets as described below, the sand was place in Teflon bags and individual particles of the aggregate were selected for analysis.

6.8.Pellet Preparation

As it is easier to handle and mount a solid sample instead of powdered sample, pellets were prepared for each powdered sample. This is possible by using the Carver Hydraulic Press (Figure 20). This machine contains a hydraulic jack which applies pressure to the powdered sample to form the pellets.

Figure 20: Carver Hydraulic Press

The powdered sample is weighed and placed in the circular mould which is inserted into the hydraulic press. At sufficient pressure (~7500 psi), the pellet (Figure 21) is formed and the gauge is released. The mass of samples taken and the mass of the corresponding pellets formed are given in Table 11. The initial and final mass of the raw materials are given in Table 12.

Table 11: Mass of Pellet Samples

Sample	Powder (g)	Teflon (g)	Teflon + Pellet (g)	Final Mass of the Pellet (g)
PS 1-1-1	0.868	0.53564	1.3833	0.84766
PS 1-1-2	0.795	0.51613	1.29282	0.77669
PS 1-1-3	0.98	0.56356	1.52737	0.96381
PS 2-1-1	0.765	0.52561	1.28479	0.75918
PS 2-1-2	0.798	0.57524	1.34257	0.76733
PS 2-1-3	0.707	0.34179	1.03452	0.69273
PS 3-1-1	0.821	0.57246	1.37601	0.80355
PS 3-1-2	0.756	0.54729	1.29624	0.74895
PS 3-1-3	0.783	0.49683	1.2743	0.77747
PS 4-1-1	0.782	0.30128	0.773	0.773
PS 4-1-2	0.861	0.57761	0.828	0.828
PS 4-1-3	0.764	0.4498	0.736	0.736

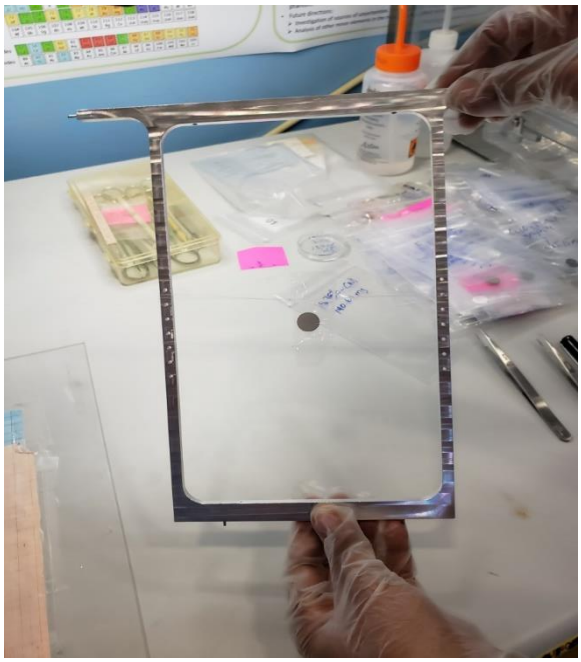

Figure 21: Pressed Pellet on a Mounting Frame

Table 12: Mass of Raw Materials

Sample	**Initial Mass (g)**	**Teflon (g)**	**Teflon + Sample (g)**	**Final Mass (g)**
Cement 1	1.088	0.716	1.375	1.017
Cement 2	1.09	0.671	1.346	1.011
Cement 3	1.058	0.551	1.295	1.019
Aggregate 1	3.118	0.439	3.548	3.118
Aggregate 2	2.339	0.662	2.738	2.339
Aggregate 3	2.235	0.626	2.422	2.235
Aggregate 4	1.996	0.649	2.199	1.996
Sand 1	1.503	0.551	1.720	1.444
Sand 2	3.856	0.757	4.087	3.835
Sand 3	4.046	0.962	4.291	3.970

6.9.Powdered Samples in PGAA

The pellets are analyzed in the cold neutron beam for their chloride content. The process is same as mentioned earlier. Each sample is kept in the beam for 1.5 hours except for the aggregates which were kept for more than 10 hours owing to low chlorine count rates. The Cl 1951 keV and Si 1273 keV count rates of each powder sample are given in Table 13.

Table 13: PGAA Data of Powdered Sample

Sample	% of Cl Conc. by weight of cement	Cl 1951 keV		Si 1273 keV	
		Counts/sec	Uncertainty %	Counts/sec	Uncertainty %
PS 1-1-1	0.20%	8.357	0.3	5.649	0.4
PS 1-1-2	0.20%	3.8	1.3	2.88	1.5
PS 1-1-3	0.20%	8.657	0.9	6.603	1
PS 2-1-1	0.10%	3.945	1.5	5.897	1
PS 2-1-2	0.10%	4.349	1.6	5.017	1.3
PS 2-1-3	0.10%	2.92	1.9	3.138	1.6
PS 3-1-1	0.01%	1.011	3.9	2.288	1.8
PS 3-1-2	0.01%	1.21	3.9	3.817	1.4
PS 3-1-3	0.01%	2.234	2.9	4.892	1.4
PS 4-1-1	Control	1.054	4.8	4.79	1.2
PS 4-1-2	Control	0.8694	4.9	4.508	1.2
PS 4-1-3	Control	0.7401	5.7	4.406	1.1

The Cl % of each sample is found from the ratio of mass of Cl at 1951 keV and mass of the pellets and is presented in Table 14 and Figure 22.

Table 14: Cl content (%) in Pellets

Sample	**% of Cl added by weight of cement**	**Position of the Beam (cm)**	**Cl (%)**
PS 1-1-1	0.2	1	0.044
PS 1-1-2	0.2	2.5	0.021
PS 1-1-3	0.2	3.6	0.039
PS 2-1-1	0.1	1	0.0245
PS 2-1-2	0.1	2.5	0.0251
PS 2-1-3	0.1	3.6	0.02
PS 3-1-1	0.01	1	0.006
PS 3-1-2	0.01	2.5	0.007
PS 3-1-3	0.01	3.6	0.013
PS 4-1-1	Control	1	0.006
PS 4-1-2	Control	2.5	0.0049
PS 4-1-3	Control	3.6	0.0047

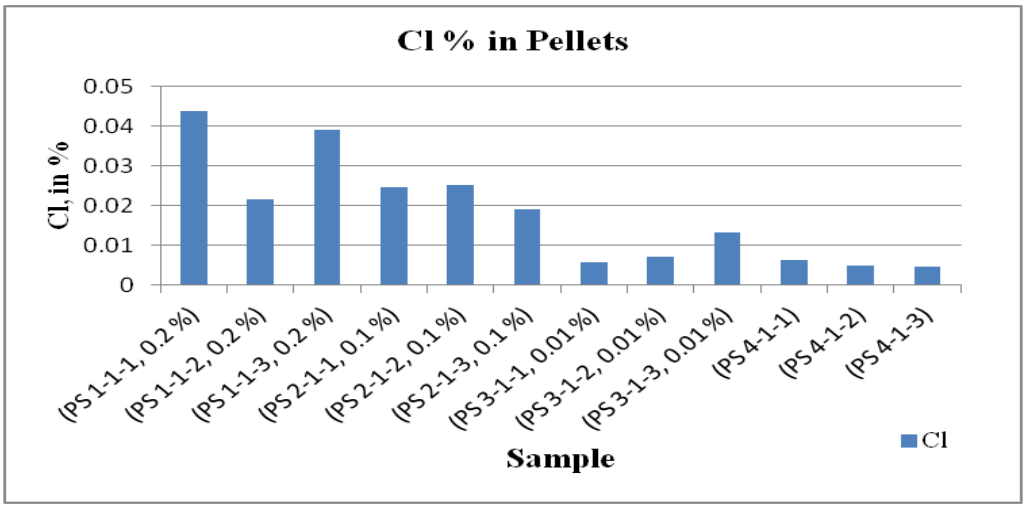

Figure 22: Cl content (%) in Pellets

The PGAA count rates for the raw materials are presented in Table 15 and the Cl % in Table 16.

Table 15: PGAA Data of Raw Materials

Sample	Cl 1951		Si 1273	
	Counts/sec	Uncertainty %	Counts/sec	Uncertainty %
Cement 1	5.126	1.5	1.617	0.6
Cement 2	3.745	2.4	1.188	0.9
Cement 3	4.475	1.7	1.508	0.7
Aggregate 1	0.4696	2.2	15.31	0.1
Aggregate 2	0.2569	5.9	4.985	0.5
Aggregate 3	0.1906	6.6	6.658	0.3
Aggregate 4	0.5211	2.4	11.48	0.2
Sand 1	0.8862	8.7	6.556	0.3
Sand 2	2.267	4.1	144	0.2
Sand 3	2	4.6	149.9	0.2

Table 16: Cl Content – Raw Materials

Sample	**Cl %**
Aggregate 1	0.00018
Aggregate 2	0.00036
Aggregate 3	0.00032
Aggregate 4	0.00099
Sand 1	0.00238
Sand 2	0.00131
Sand 3	0.00101
Cement 1	0.02066
Cement 2	0.01685
Cement 3	0.01909

CHAPTER 7: DISCUSSION

7.1.Chloride Percentage from Each Method

The average chloride percentage of the intact samples for each batch is given in Table 17 and Figure 23.

Table 17: Mean Cl % by weight of cement – Cylinders

Batch	Cl %
0.20%	0.2128
0.10%	0.112
0.01%	0.0268
Control	0.0363

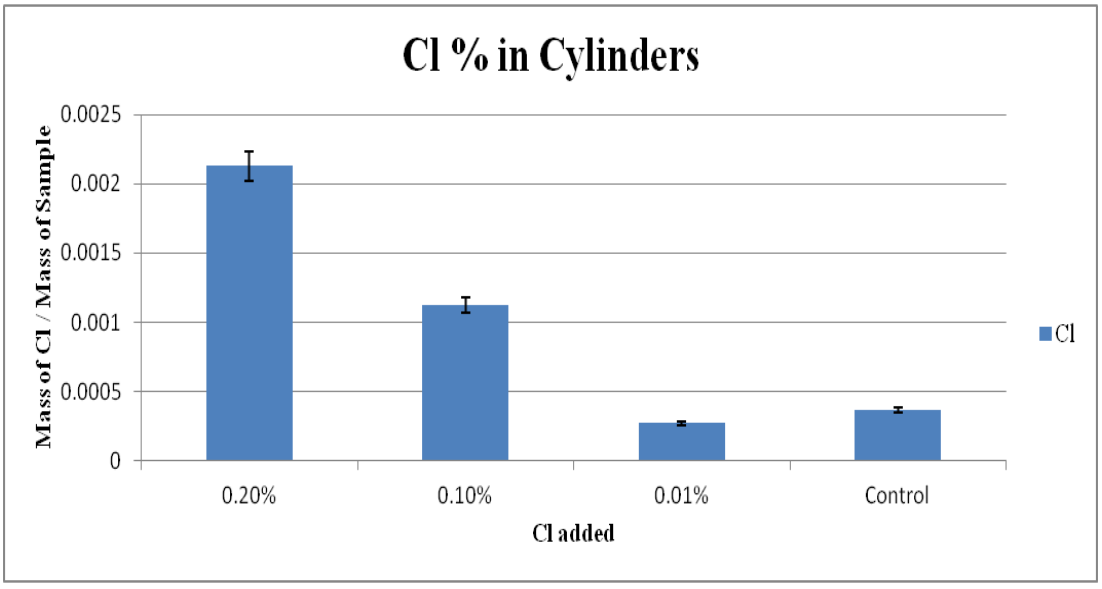

Figure 23: Cl % in Cylinders based on Mass

From the above data, when considering the mass of the sample and mass of Cl 1951, the chloride percentage in control samples is higher than the samples containing

0.01% added chloride. However, when comparing the area of Cl and area of Si (Figure 24), the chloride percentage of each batch fits our pattern of initial added chloride. This shows that PGAA provides us data in varied parallels that help us understand the results better.

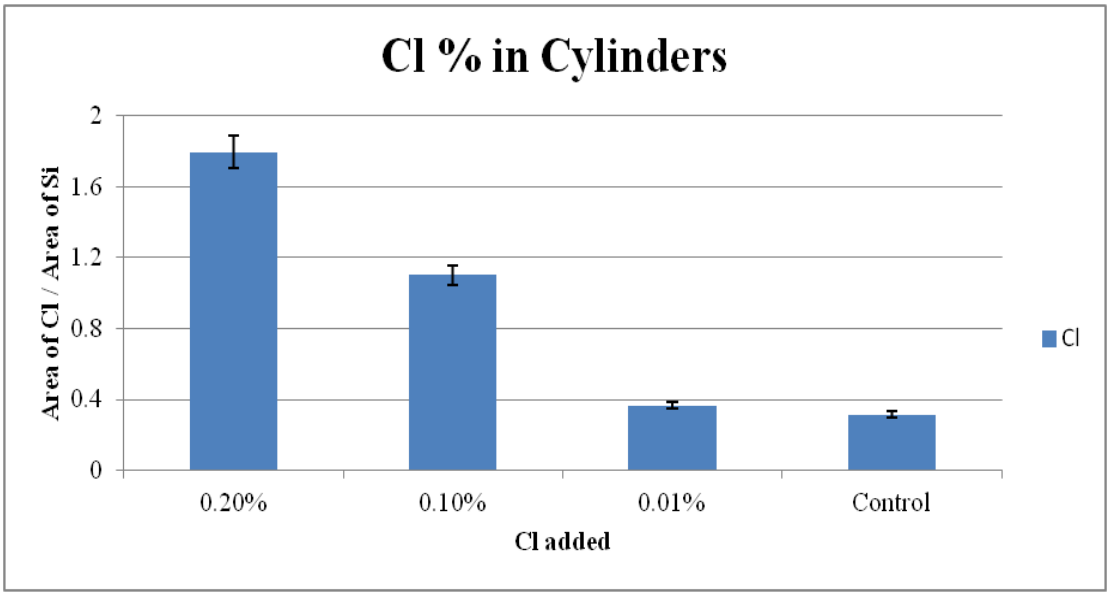

Figure 24: Cl % in Cylinders based on Area

Similarly, the mean chloride percentage of each batch obtained from the powdered samples using C1152 and PGAA are given in Table 18 and Table 19.

Table 18: Mean Cl % -C1152

Batch	**Cl %**
0.20%	0.03813
0.10%	0.0248
0.01%	0.0189
Control	-0.0131

Table 19: Mean Cl % - Pellets

Batch	Cl %
0.20%	0.034847
0.10%	0.02292
0.01%	0.008732
Control	0.005223

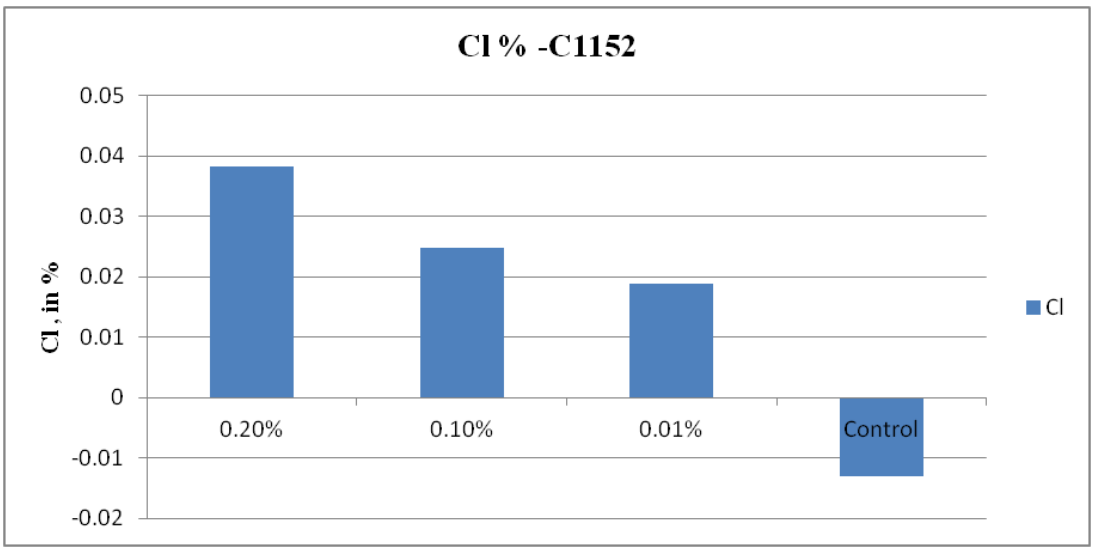

Figure 25: Mean Cl content (%) -C1152

The negative sign in the chloride value of control samples (Figure 25) confirms our initial assumption that the chloride levels were beyond the scope of the instrument. This shows that this method is not suitable for conditions where the chloride limit is very low.

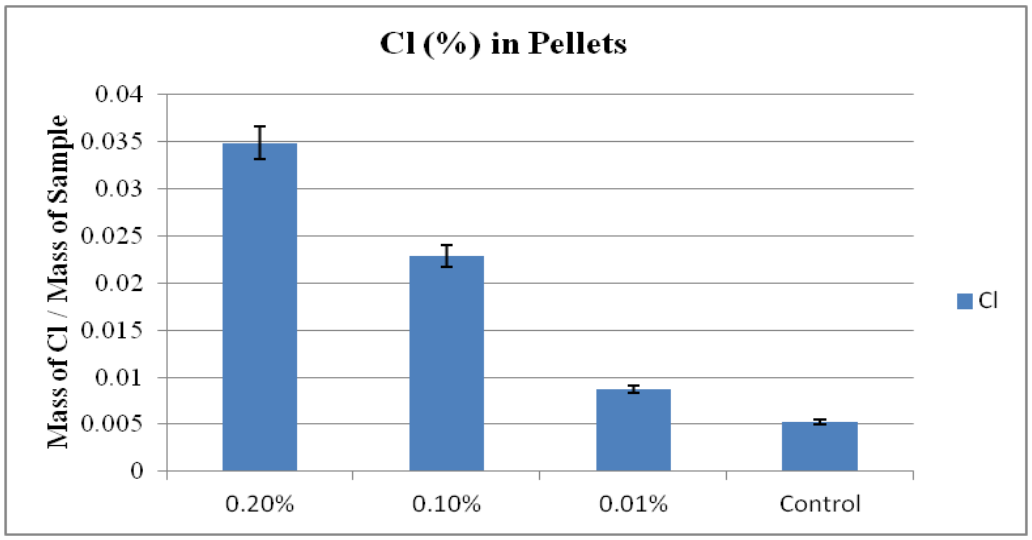

Figure 26: Mean Cl content (%) - Pellets

From Figure 26, it is clear that the PGAA of powdered samples gives more accurate results of the chloride percentage in concrete when compared to C1152, without altering the initial sample. The mean chloride percentage for the raw materials is calculated by the same method and the corrected values are presented in Table 20. A graphical representation is shown in Figure 27.

Table 20: Raw Materials-Linearity Correction

Sample	**Cl %**
Aggregate	0.00047 ± 0.00031
Sand	0.001565 ± 0.000587
Cement	0.018865 ± 0.00156

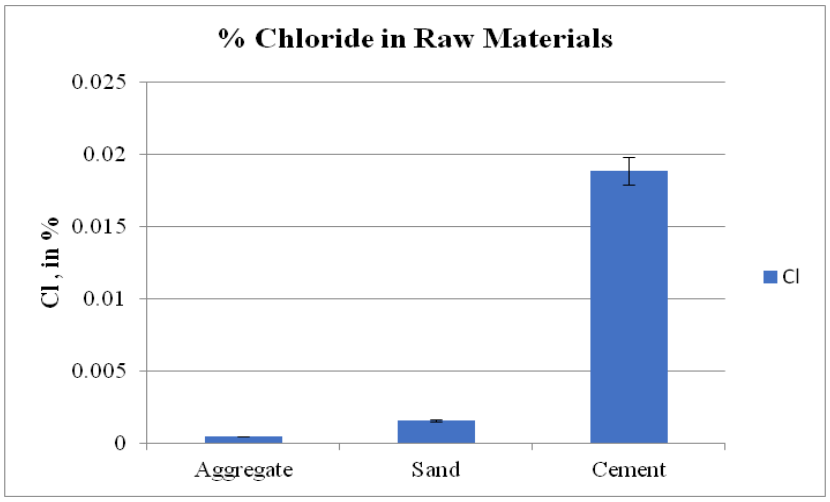

Figure 27: Chloride content (%) in Raw Materials

7.2.Comparison of Results

The chloride percentage measured from NDT PGAA and ASTM C1152 is corrected and plotted for each batch. Figure 28 shows that PGAA of intact samples has better linearity when compared to the powdered testing.

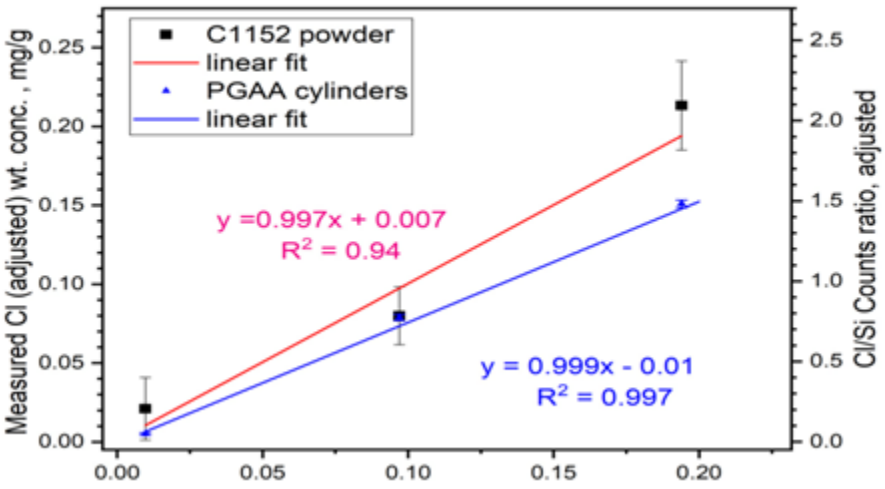

% of Cl added by weight of cement

Figure 28: NDT PGAA vs. C1152

The plot is reasonably good, given the scatter in the data. This illustrates that measuring the chloride content using PGAA provides excellent results without

destroying the structure. Similarly, the chloride percentage for the powdered samples found in C1152 and PGAA are plotted in Figure 29.

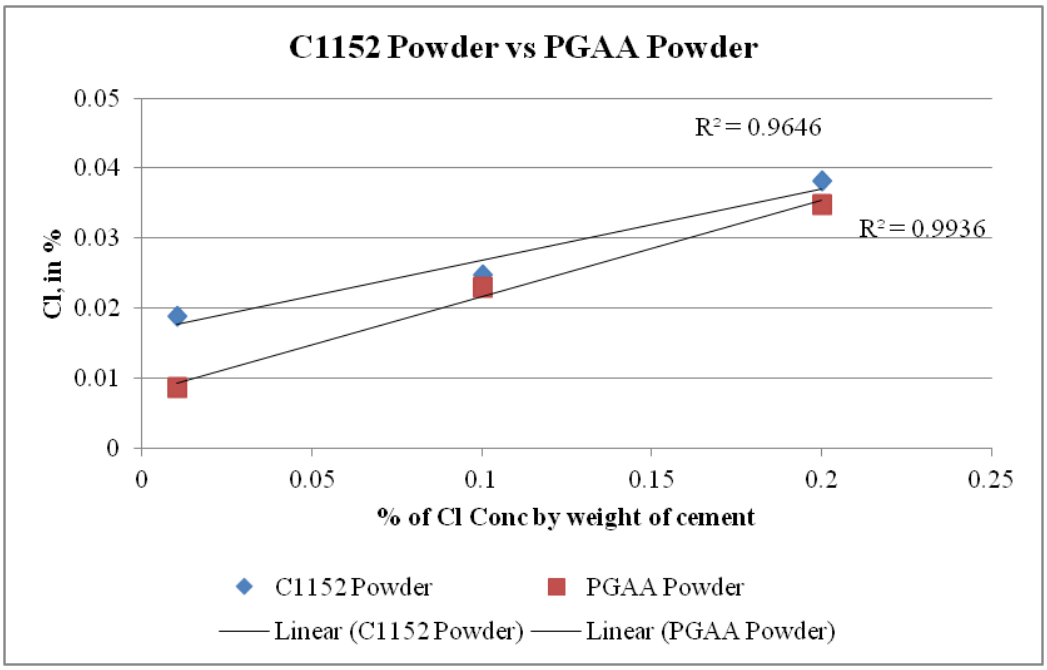

Figure 29: C1152 powder vs. PGAA Powder

The plot shows very good agreement for the results obtained from C1152 and PGAA for the powdered samples. Even then, the fit of PGAA is more linear than C1152. This shows that the PGAA method overall is a better method than C1152.

CHAPTER 8: CONCLUSIONS AND FUTURE RESEARCH

This study aimed to compare the performance of a neutron-based nondestructive testing method, Prompt Gamma Activation Analysis (PGAA) against the destructive wet chemistry method ASTM C-1152 currently used to determine the chloride concentration in concrete. The following conclusions were made based on this study:

- The PGAA method is capable of detecting Cl at levels corresponding to the corrosion threshold of 0.1-0.2% Cl by weight of cement.
- The minimum detectable limit for PGAA is below 0.02% Cl by weight of cement and approaches the Cl background contributed by the raw materials, in this case mainly the cement.
- The PGAA-measured chloride concentrations showed excellent linearity after correction for the chloride content in the concrete raw materials.
- For the powdered samples, the C1152 and PGAA results were in very good agreement. However, the PGAA data showed much less scatter with an uncertainty as low as 0.3%.
- C1152 is not reliable to test lower levels of chloride in concrete.
- PGAA can be performed on intact specimens and reduces time by avoiding crushing, sieving and nitric acid extraction. Hence, it is a feasible replacement for the C1152 method.
- PGAA can be used to study the composition of raw materials, and measure the chloride ingress based on the weight of cement instead of by weight of chloride.

Future research could include:

- Preparing and testing concrete specimens with gradients of Cl emplaced in them, in order to determine the spatial resolution of the PGAA slit collimation method.
- Applying Monte Carlo neutron and gamma-ray transport software to evaluate the effects of neutron and gamma-ray attenuation within the intact specimens on the accuracy of PGAA method.
- Designing, building and testing a standalone PGAA chloride measurement system based on a neutron generator rather than a reactor-based neutron beam.
- Developing a portable PGAA measurement system that can be used in the field to measure chlorides in actual concrete structures without taking cores.

APPENDIX

PeakEasy Post Processed data

Table 21: PeakEasy Output- Pellet (0.2% -1 cm)

S.No	Energy	Nuclide	Mass (mg)	Relative Unc.	Unc.	File
1	846.8	S-33	4.963	0.00157	0.008	PS-1-1-1- Pellet
2	3220.98	S-33	1.112	0.01856	0.021	PS-1-1-1- Pellet
3	5421.52	S-33	0.918	0.01298	0.012	PS-1-1-1- Pellet
4	1164.82	Cl-36	0.391	0.00123	0.001	PS-1-1-1- Pellet
5	1951.38	Cl-36	0.372	0.00203	0.001	PS-1-1-1- Pellet
6	1959.61	Cl-36	0.381	0.00284	0.001	PS-1-1-1- Pellet
7	6112.01	Cl-36	0.402	0.00316	0.001	PS-1-1-1- Pellet
8	1273.5	Si-29	33.276	0.00256	0.085	PS-1-1-1- Pellet
9	3539.76	Si-29	26.485	0.00168	0.044	PS-1-1-1- Pellet
10	1942.91	Ca-41	172.577	0.00033	0.057	PS-1-1-1- Pellet
11	2001.58	Ca-41	154.002	0.00096	0.147	PS-1-1-1- Pellet
12	6420.77	Ca-41	183.527	0.00081	0.149	PS-1-1-1- Pellet

Table 22: PeakEasy Output- Pellet (0.2% -2.5 cm)

S.No	Energy	Nuclide	Mass (mg)	Relative Unc.	Unc.	File
1	846.82	S-33	0.580	0.019	0.011	PS-1-1-2- Pellet
2	3220.9	S-33	0.632	0.071	0.045	PS-1-1-2- Pellet
3	5421.5	S-33	0.526	0.049	0.026	PS-1-1-2- Pellet
4	1164.9	Cl-36	0.172	0.006	0.001	PS-1-1-2- Pellet
5	1951.4	Cl-36	0.167	0.009	0.002	PS-1-1-2- Pellet
6	1959.7	Cl-36	0.189	0.012	0.002	PS-1-1-2- Pellet
7	6112.1	Cl-36	0.178	0.015	0.003	PS-1-1-2- Pellet
8	1273.5	Si-29	16.751	0.011	0.188	PS-1-1-2- Pellet
9	3539.8	Si-29	13.592	0.007	0.097	PS-1-1-2- Pellet
10	1942.9	Ca-41	91.983	0.001	0.127	PS-1-1-2- Pellet
11	2001.6	Ca-41	82.740	0.004	0.329	PS-1-1-2- Pellet
12	6420.8	Ca-41	98.033	0.003	0.333	PS-1-1-2- Pellet

Table 23: PeakEasy Output- Pellet (0.2% -3.6 cm)

S.No	Energy	Nuclide	Mass (mg)	Relative Unc.	Unc.	File
1	846.79	S-33	1.388	0.012	0.017	PS-1-1-3- Pellet
2	3220.94	S-33	1.911	0.037	0.071	PS-1-1-3- Pellet
3	5421.56	S-33	1.481	0.028	0.041	PS-1-1-3- Pellet
4	1164.81	Cl-36	0.413	0.004	0.002	PS-1-1-3- Pellet
5	1951.37	Cl-36	0.386	0.006	0.002	PS-1-1-3- Pellet
6	1959.58	Cl-36	0.393	0.009	0.004	PS-1-1-3- Pellet
7	6112	Cl-36	0.437	0.009	0.004	PS-1-1-3- Pellet
8	1273.5	Si-29	38.256	0.007	0.282	PS-1-1-3- Pellet
9	3539.75	Si-29	31.016	0.005	0.145	PS-1-1-3- Pellet
10	1942.91	Ca-41	202.362	0.001	0.187	PS-1-1-3- Pellet
11	2001.57	Ca-41	180.306	0.003	0.490	PS-1-1-3- Pellet
12	6420.75	Ca-41	216.015	0.002	0.489	PS-1-1-3- Pellet

Table 24: PeakEasy Output- Pellet (0.1% -1 cm)

S.No	Energy	Nuclide	Mass (mg)	Relative Unc.	Unc.	File
1	847.15	S-33	1.367	0.011	0.016	PS-2-1-1- Pellet
2	3221.44	S-33	1.785	0.036	0.064	PS-2-1-1- Pellet
3	5421.86	S-33	1.481	0.024	0.0358	PS-2-1-1- Pellet
4	1165.17	Cl-36	0.199	0.006	0.001	PS-2-1-1- Pellet
5	1951.72	Cl-36	0.186	0.011	0.002	PS-2-1-1- Pellet
6	1959.94	Cl-36	0.187	0.016	0.003	PS-2-1-1- Pellet
7	6112.36	Cl-36	0.196	0.015	0.003	PS-2-1-1- Pellet
8	1273.85	Si-29	35.257	0.007	0.253	PS-2-1-1- Pellet
9	3540.12	Si-29	29.708	0.004	0.131	PS-2-1-1- Pellet
10	1943.26	Ca-41	170.825	0.001	0.160	PS-2-1-1- Pellet
11	2001.93	Ca-41	150.176	0.003	0.423	PS-2-1-1- Pellet
12	6421.08	Ca-41	179.537	0.002	0.413	PS-2-1-1- Pellet

Table 25: PeakEasy Output- Pellet (0.1% -2.5 cm)

S.No	Energy	Nuclide	Mass (mg)	Relative Unc.	Unc.	File
1	846.81	S-33	0.921	0.017	0.0158	PS-2-1-2- Pellet
2	3221.01	S-33	1.298	0.051	0.0668	PS-2-1-2- Pellet
3	5421.47	S-33	0.980	0.039	0.0385	PS-2-1-2- Pellet
4	1164.82	Cl-36	0.206	0.006	0.001	PS-2-1-2- Pellet
5	1951.35	Cl-36	0.193	0.011	0.002	PS-2-1-2- Pellet
6	1959.6	Cl-36	0.193	0.016	0.003	PS-2-1-2- Pellet
7	6112.01	Cl-36	0.214	0.016	0.003	PS-2-1-2- Pellet
8	1273.54	Si-29	29.088	0.009	0.274	PS-2-1-2- Pellet
9	3539.75	Si-29	21.467	0.006	0.133	PS-2-1-2- Pellet
10	1942.9	Ca-41	180.462	0.001	0.192	PS-2-1-2- Pellet
11	2001.57	Ca-41	160.697	0.003	0.497	PS-2-1-2- Pellet
12	6420.74	Ca-41	190.366	0.003	0.499	PS-2-1-2- Pellet

Table 26: PeakEasy Output- Pellet (0.1% -3.6 cm)

S.No	Energy	Nuclide	Mass (mg)	Relative Unc.	Unc.	File
1	846.83	S-33	0.643	0.020	0.013	PS-2-1-3- Pellet
2	3220.92	S-33	0.944	0.057	0.054	PS-2-1-3- Pellet
3	5421.62	S-33	0.579	0.051	0.029	PS-2-1-3- Pellet
4	1164.83	Cl-36	0.139	0.007	0.001	PS-2-1-3- Pellet
5	1951.39	Cl-36	0.132	0.012	0.002	PS-2-1-3- Pellet
6	1959.61	Cl-36	0.136	0.018	0.002	PS-2-1-3- Pellet
7	6112.02	Cl-36	0.142	0.019	0.003	PS-2-1-3- Pellet
8	1273.55	Si-29	18.562	0.012	0.216	PS-2-1-3- Pellet
9	3539.74	Si-29	13.471	0.008	0.103	PS-2-1-3- Pellet
10	1942.92	Ca-41	125.272	0.001	0.155	PS-2-1-3- Pellet
11	2001.6	Ca-41	112.393	0.006	0.399	PS-2-1-3- Pellet
12	6420.75	Ca-41	131.091	0.003	0.400	PS-2-1-3- Pellet

Table 27: PeakEasy Output- Pellet (0.01% -1 cm)

S.No	Energy	Nuclide	Mass (mg)	Relative Unc.	Unc.	File
1	846.86	S-33	0.475	0.022	0.01	PS-3-1-1- Pellet
2	3221.07	S-33	0.657	0.066	0.043	PS-3-1-1- Pellet
3	5421.69	S-33	0.532	0.047	0.025	PS-3-1-1- Pellet
4	1164.85	Cl-36	0.047	0.014	0.001	PS-3-1-1- Pellet
5	1951.36	Cl-36	0.047	0.025	0.001	PS-3-1-1- Pellet
6	1959.62	Cl-36	0.043	0.043	0.002	PS-3-1-1- Pellet
7	6112.08	Cl-36	0.044	0.04	0.002	PS-3-1-1- Pellet
8	1273.57	Si-29	13.299	0.013	0.175	PS-3-1-1- Pellet
9	3539.79	Si-29	10.004	0.009	0.086	PS-3-1-1- Pellet
10	1942.94	Ca-41	84.624	0.001	0.124	PS-3-1-1- Pellet
11	2001.61	Ca-41	76.523	0.004	0.321	PS-3-1-1- Pellet
12	6420.81	Ca-41	89.484	0.004	0.322	PS-3-1-1- Pellet

Table 28: PeakEasy Output- Pellet (0.01% -2.5 cm)

S.No	Energy	Nuclide	Mass (mg)	Relative Unc.	Unc.	File
1	846.79	S-33	0.812	0.017	0.014	PS-3-1-2- Pellet
2	3220.92	S-33	0.925	0.062	0.057	PS-3-1-2- Pellet
3	5421.55	S-33	0.793	0.041	0.033	PS-3-1-2- Pellet
4	1164.82	Cl-36	0.053	0.015	0.001	PS-3-1-2- Pellet
5	1951.37	Cl-36	0.053	0.028	0.001	PS-3-1-2- Pellet
6	1959.61	Cl-36	0.048	0.048	0.002	PS-3-1-2- Pellet
7	6111.95	Cl-36	0.053	0.044	0.002	PS-3-1-2- Pellet
8	1273.54	Si-29	22.071	0.011	0.233	PS-3-1-2- Pellet
9	3539.73	Si-29	15.994	0.007	0.111	PS-3-1-2- Pellet
10	1942.89	Ca-41	148.049	0.001	0.168	PS-3-1-2- Pellet
11	2001.56	Ca-41	132.48	0.003	0.432	PS-3-1-2- Pellet
12	6420.7	Ca-41	157.309	0.003	0.438	PS-3-1-2- Pellet

Table 29: PeakEasy Output- Pellet (0.01% -3.6 cm)

S.No	Energy	Nuclide	Mass (mg)	Relative Unc.	Unc.	File
1	846.77	S-33	1.001	0.016	0.016	PS-3-1-3- Pellet
2	3220.91	S-33	1.147	0.059	0.067	PS-3-1-3- Pellet
3	5421.47	S-33	0.882	0.043	0.038	PS-3-1-3- Pellet
4	1164.81	Cl-36	0.112	0.01	0.001	PS-3-1-3- Pellet
5	1951.34	Cl-36	0.104	0.018	0.002	PS-3-1-3- Pellet
6	1959.61	Cl-36	0.106	0.028	0.003	PS-3-1-3- Pellet
7	6111.92	Cl-36	0.112	0.027	0.003	PS-3-1-3- Pellet
8	1273.53	Si-29	28.522	0.01	0.278	PS-3-1-3- Pellet
9	3539.74	Si-29	22.289	0.006	0.136	PS-3-1-3- Pellet
10	1942.88	Ca-41	190.098	0.001	0.198	PS-3-1-3- Pellet
11	2001.55	Ca-41	169.306	0.003	0.51	PS-3-1-3- Pellet
12	6420.72	Ca-41	202.336	0.003	0.517	PS-3-1-3- Pellet

Table 30: PeakEasy Output- Pellet (Control -1 cm)

S.No	Energy	Nuclide	Mass (mg)	Relative Unc.	Unc.	File
1	846.86	S-33	0.967	0.015	0.015	PS 4-1-1 Pellet
2	3221.18	S-33	1.221	0.05	0.061	PS 4-1-1 Pellet
3	5421.82	S-33	0.961	0.037	0.036	PS 4-1-1 Pellet
4	1164.91	Cl-36	0.054	0.016	0.001	PS 4-1-1 Pellet
5	1951.55	Cl-36	0.048	0.032	0.002	PS 4-1-1 Pellet
6	1959.74	Cl-36	0.053	0.049	0.003	PS 4-1-1 Pellet
7	6112.4	Cl-36	0.05	0.049	0.002	PS 4-1-1 Pellet
8	1273.63	Si-29	27.73	0.009	0.247	PS 4-1-1 Pellet
9	3540.01	Si-29	20.89	0.006	0.122	PS 4-1-1 Pellet
10	1943.04	Ca-41	188.346	0.001	0.183	PS 4-1-1 Pellet
11	2001.72	Ca-41	167.393	0.003	0.464	PS 4-1-1 Pellet
12	6421.2	Ca-41	196.066	0.002	0.472	PS 4-1-1 Pellet

Table 31: PeakEasy Output- Pellet (Control -2.5 cm)

S.No	Energy	Nuclide	Mass (mg)	Relative Unc.	Unc.	File
1	846.86	S-33	0.967	0.014	0.014	PS 4-1-2 Pellet
2	3221.17	S-33	1.099	0.052	0.057	PS 4-1-2 Pellet
3	5421.91	S-33	0.88	0.036	0.032	PS 4-1-2 Pellet
4	1164.91	Cl-36	0.043	0.018	0.001	PS 4-1-2 Pellet
5	1951.45	Cl-36	0.04	0.035	0.001	PS 4-1-2 Pellet
6	1959.7	Cl-36	0.041	0.056	0.002	PS 4-1-2 Pellet
7	6112.42	Cl-36	0.038	0.058	0.002	PS 4-1-2 Pellet
8	1273.62	Si-29	26.485	0.009	0.233	PS 4-1-2 Pellet
9	3540.01	Si-29	19.886	0.006	0.114	PS 4-1-2 Pellet
10	1943.03	Ca-41	180.462	0.001	0.171	PS 4-1-2 Pellet
11	2001.71	Ca-41	159.741	0.003	0.432	PS 4-1-2 Pellet
12	6421.19	Ca-41	188.657	0.002	0.441	PS 4-1-2 Pellet

Table 32: PeakEasy Output- Pellet (Control -3.6 cm)

S.No	Energy	Nuclide	Mass (mg)	Relative Unc.	Unc.	File
1	846.87	S-33	1.245	0.01	0.013	PS 4-1-3 Pellet
2	3221.2	S-33	0.931	0.052	0.049	PS 4-1-3 Pellet
3	5421.97	S-33	0.87	0.033	0.029	PS 4-1-3 Pellet
4	1164.93	Cl-36	0.04	0.017	0.001	PS 4-1-3 Pellet
5	1951.49	Cl-36	0.034	0.036	0.001	PS 4-1-3 Pellet
6	1959.8	Cl-36	0.032	0.063	0.002	PS 4-1-3 Pellet
7	6111.38	Cl-36	0.02	0.081	0.002	PS 4-1-3 Pellet
8	1273.63	Si-29	25.579	0.008	0.202	PS 4-1-3 Pellet
9	3540.04	Si-29	19.248	0.005	0.1	PS 4-1-3 Pellet
10	1943.06	Ca-41	166.445	0.001	0.146	PS 4-1-3 Pellet
11	2001.73	Ca-41	150.654	0.003	0.377	PS 4-1-3 Pellet
12	6421.26	Ca-41	171.558	0.002	0.375	PS 4-1-3 Pellet

REFERENCES

1. AASHTO T 277 (2007). Standard method of test for electrical indication of concrete's ability to resist chloride ion penetration, 2007.
2. A. Costa and J. Appleton, Concrete Carbonation and Chloride Penetration in a Marine Environment, Concrete Science and Engineering, Vol. 3, pp 242-249, December 2001.
3. Adam Neville, Chloride Attack of Reinforced Concrete: An Overview, Journal of Materials and Structures, Issue 28, pp 63-70, 1995.
4. ASTM C 672, Standard Test Method for Scaling Resistance of Concrete Surfaces Exposed to Deicing Chemicals, ASTM, 2012.
5. ASTM C 1202, Standard Test Method for Electrical Indication of Concrete's Ability to Resist Chloride Ion Penetration, 2012.
6. Building Code Portal, ACI 318, American Concrete Institute, 2014.
7. CEN/TS 12390-9, Testing of Hardened Concrete, 2006.
8. Corrosion of Metals in Concrete, ACI 222R-96, American Concrete Institute, 1996.
9. Elyson A. P. Liberati, Caio Gorla Nogueira, Edson Denner Leonel, Alaa Chateauneuf, Failure Analysis of Reinforced Concrete Structures Subjected to Chloride Penetration and Reinforcements Corrosion, Research Gate, DOI: 10.1016/B978-0-08-100116-5.00005-3, December 2016.
10. Hongfei Zhang, Weiping Zhang, Xianglin Gu, Xianyu Jin, Nanguo Jin, Chloride Penetration in Concrete under Marine Atmospheric Environment –

Analysis of the Influencing Factors, Journal of Structure and Infrastructure Engineering Maintenance, Management, Life-Cycle Design and Performance Volume 12, Issue 11, 2016.

11. https://en.wikipedia.org/wiki/Cement_accelerator
12. https://www.concretedecor.net/decorativeconcretearticles/vol-5-no-5-octnov-2005/mixtures-and-additives-accelerating-admixtures/
13. https://www.cement.org/learn/concrete-technology/concrete-construction/curing-in-construction
14. http://web.mit.edu/parmstr/Public/NRCan/CanBldgDigests/cbd165_e.html
15. https://theconstructor.org/concrete/chloride-attack-concrete-structures-cause-prevention/7802/
16. https://en.wikipedia.org/wiki/Semiconductor_detector
17. https://www.thebalance.com/what-is-spalling-1798631
18. https://www.concreteconstruction.net/how-to/what-caused-this-scaling-1_o
19. https://www.concretenetwork.com/concrete-delamination.html
20. K.D. Stanish, R.D. Hooton and M.D.A. Thomas, Testing the Chloride Penetration Resistance of Concrete: A Literature Review, Department of Civil Engineering University of Toronto, Toronto, Ontario, Canada
21. McGrath. P. Development of Test Methods for Predicting Chloride Penetration into High Performance Concrete, 1996, Ph.D. Thesis, Department of Civil Engineering, University of Toronto.

22. Mobasher, B. and Mitchell, T.M., “Laboratory Experience with the Rapid Chloride Permeability Test”, ACI SP-108: Permeability of Concrete, (ed. D. Whiting, A. Walitt), American Concrete Institute, 1988.
23. NGD cold-neutron prompt gamma-ray activation analysis spectrometer at NIST, Journal of Radioanalytical and Nuclear Chemistry, April 2015, Volume 304, Issue 1, pp 189–193.
24. Standard Test Method for Acid-Soluble Chloride in Mortar and Concrete, ASTM International, C1152/C1152M − 04 (Reapproved 2012).
25. Teresa Zych, Test Methods of Concrete Resistance to Chloride Ingress
26. Ueli Angst, Bernhard Elsener, Claus K. Larsen, Øystein Vennesland, Critical chloride content in reinforced concrete — A review, Cement and Concrete Research 39 (2009) 1122–1138.
27. Y. Zhou; B. Gencturk, A.M.ASCE; K. Willam, F.ASCE; and A. Attar, Carbonation-Induced and Chloride-Induced Corrosion in Reinforced Concrete Structures, Journal of Materials in Civil Engineering, Volume 27, Issue 9, September 2015.
28. Whiting, D., “Rapid Measurement of the Chloride Permeability of Concrete”, Public Roads, Vol. 45, No. 3, pp. 101-112, 1981
29. Zenonas Kamaitis, Damage to concrete bridges due to reinforcement corrosion, Transport, 2002, 17:4, 137-142